KUNGL. TEKNISKA HÖGSKOLANS HANDLINGAR

TRANSACTIONS OF THE ROYAL INSTITUTE OF TECHNOLOGY
STOCKHOLM, SWEDEN

Nr 148 1959

Electrical Engineering 3

UDC 621.318.435.3

SELF-SUSTAINED MODULATIONS IN TRANSDUCTOR CIRCUITS WITH SERIES CAPACITORS

BY

F. DAHLGREN and R. ŁADZIŃSKI

STOCKHOLM
AB HENRIK LINDSTÄHLS BOKHANDEL I DISTRIBUTION

Forts. fr. omsl. 3:dje sida.

132. Schlyter, Kurt, *A Precision Calorimeter for Enthalpy Titrations.* (Chem. 2) 41 s. 1959. Kr. 5: —.
133. Laurent, Torbern, *Zig-zag filters.* (El. Engng. 1) 58 s. 1959. Kr. 7: —.
134. Lamm, Ole, *Dynamical Principles Applied to the Sedimentation Diffusion Processes at Finite Concentrations.* (Chem. 3) 21 s. 1959. Kr. 3: —.
135. Laurent, Torbern, *Filter Calculations Using the Template Method.* (El. Engng. 2) 30 s. 1959. Kr. 4: —.
136. Hult, Jan, *Creep Buckling of Plane Frameworks.* (Mech. Engng. 1) 31 s. 1959. Kr. 4: —.
137. Janson, Lars-Eric, *Evaporation from Salt Water in Arid Zones.* (Civil Engng. 1) 14 s. 1959. Kr. 2: —.
138. Bjerninger, Sigfrid, *Investigations into Braking of Tractors and Trailers.* (Mech. Engng. 2) 136 s. 1959. Kr. 12: 50.
139. Broberg, K. B., *A Problem on Stress Waves in an Infinite Elastic Plate.* (Mech. Engng. 3) 27 s. 1959. Kr. 3: 50.
140. Hallert, B. — Ottoson, L., *General Differential Formulae of the Complete Projective Relations Between Planes.* (Arch., Build., Surv. 1). 15 s. 1959. Kr. 2: —.
141. Andersson, Bengt Joel, *On Planing Boats.* (Aeron. Shipb. 1) 30 s. 1959. Kr. 4: 50.
142. Ljunggren, Stig, *A Study of Electrodiffusion and of Diffusion Combined with Kinetics, by Means of Moment Analysis.* (Chem. 4) 24 s. 1959. Kr. 3: 50.
143. Engstrand, Georg, *Use of Radioactive Isotopes for Measurement of Cutting Tool Wear.* (Mech. Engng. 4) 18 s. 1959. Kr. 2: 50.
144. Engstrand, Georg, *Does Compensation of Thermoelectric Currents Influence Cutting Tool Wear.* (Mech. Engng. 5) 12 s. 1959. Kr. 1: 50.
145. Holmberg, Bengt R., *On the Elimination of the Barycentric and Rotational Coordinates in a Nuclear »Shell-Model».* (Math. & Phys. 1) 28 s. 1959. Kr. 4: —.
146. Hellström, B., and Janson, L.-E., *Evaporation from Water Surfaces Coated with a Film of Stearyl Alcohol.* (Civil Engng. 2) 18 s. 1959. Kr. 2: 50.
147. Larsson, Gerhard, *Studies on Forest Road Planning.* (Arch. Build. Surv. 2) 137 s. 1959. Kr. 13: —.
148. Dahlgren, F., and Ładziński, R., *Self-sustained Modulations in Transductor Circuits with Series Capacitors.* (El. Engng. 3) 64 s. 1959. Kr. 7: 50.

Pris kronor 7: 50

ELANDERS BOKTRYCKERI AB. GÖTEBORG 1959

KUNGL. TEKNISKA HÖGSKOLANS HANDLINGAR

TRANSACTIONS OF THE ROYAL INSTITUTE OF TECHNOLOGY
STOCKHOLM, SWEDEN

Nr 148 1959

Electrical Engineering 3

UDC 621.318.435.3

SELF-SUSTAINED MODULATIONS IN TRANSDUCTOR CIRCUITS WITH SERIES CAPACITORS

BY

F. DAHLGREN and R. ŁADZIŃSKI

GÖTEBORG 1959
ELANDERS BOKTRYCKERI AKTIEBOLAG

Summary

Transductors with series capacitors in the a. c. circuits create, under certain conditions, amplitude modulations of all electrical quantities in the circuits involved. A contribution to the understanding of this phenomenon is presented, as well as confirming experimental results.

I. Introduction

Transductors in combination with capacitors in their a. c. circuits are used for several practical applications. As an example may be mentioned such transductor combinations, utilized for instance in power regulating circuits, where the transductor is intended to act like an underexited synchronous motor with very low transient reactance. This very low reactance is obtained by means of a series capacitor, which compensates the predominant part of the leakage reactance. Another example is an equipment for a. c. welding, either by 50 Hz or by the use of tripling elements for 150 Hz, in both cases using d. c. excitation for regulating purposes, which means that the magnetic elements to a certain extent act as transductors.

Experimental investigations in the two mentioned fields of transductor applications have shown that the combination transductor-capacitor often creates a modulation phenomenon which changes their whole performance. In the former example mentioned above this phenomenon is evidently far from desirable. In the latter case, however, it may open possibilities for static generation of such modulations which are now deliberately generated by rotating machinery for certain types of welding equipment. Another field of application where self-sustained modulations may be utilized, is intermittent illumination, e. g. for signals, signs and show-windows.

It is obvious that a closer investigation of the nature and laws of this phenomenon is greatly desirable whether the purpose is to suppress or utilize the same.

The modulation referred to consists of an oscillation of the amplitude of voltage and current with a frequency of the order of magnitude 1 to 5 complete cycles per second. It must be clearly pointed out that the phenomenon means a real amplitude modulation and not a set of subharmonics. The general type of this modulation is shown by for instance the oscillogram fig. 37 page 51.

Several modes of connection of the transductor and capacitor are possible. Some of these have been mentioned in the literature, in connection with a statement of the occurrence of a modulation, but a closer investigation of the nature of the process does not seem to have been published. It should also be emphasized that the phenomenon dealt with here is altogether different from that which is due to a capacitor in the *excitation* circuit, such as is used in practice for certain intermittent lighting devices. This latter phenomenon will be dealt with quite briefly towards the end of this paper.

II. Fundamental considerations

II.1 Basic assumptions and harmonic components

The general discussion and theoretical treatment presented in the following are based on certain simplifying assumptions and approximations, which are necessary to make it possible to deal with the processes in a clear and mathematically correct manner. These simplifications, which are by far not unreasonable, can be summarized as follows:

1. The transductor is a parallel transductor without self-excitation.
2. The resistance and leakage inductance of its a. c. windings are neglected, as well as its active core losses. No hysteresis loop is thus assumed.
3. The exterior a. c. circuit contains a source of sinusoidal voltage, and a resistor and a capacitor in series.
4. The d. c. circuit contains an exterior source of d. c. voltage, and a certain resistance, while the leakage and exterior inductances are neglected.

Due to the parallel connection, and the resistance and leakage inductance of the a. c. windings being negligible, the transductor operates under the conditions of "natural excitation" or "free current

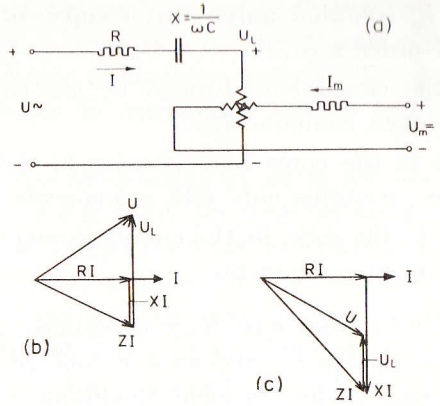

Fig. 1. General diagram of circuit, and phasor diagrams.

operation", see IEC International Electrotechnical Vocabulary, group 12.

The general diagram of connections of the circuit are shown in fig. 1 a, which also gives the fundamental notations used in the following. See also fig. 8 a, relating to the special case of parallel transductor.

As a base for the general treatment of the processes in the transductor it might be useful to give a brief summary of some wellknown facts related to the flux and current harmonics occurring in the windings of a transductor having only two windings, one of them supplied from an a. c. source, the other from a d. c. source. As hysteresis and other losses are neglected all time curves must be symmetrical around vertical axis' through the centers of the half waves. From this fact, in conjunction with the assumed symmetry of the elements and circuits, the following rules are easily derived, all referring to the reference directions defined in fig. 8 a.

1. The fluxes Φ_1 och Φ_2 contain both odd and even components. The even components are in phase and the odd components in counterphase in the two cores. Among the even components is included the component or order zero.
2. The currents i_1 och i_2 contain both odd and even components. The even components are in counterphase and the odd components in phase in the two a. c. windings. Consequently, the exterior current $i = i_1 + i_2$ contains only odd components.

3. The current i_m contains only even components, including the component of order zero.
4. The emf in the closed loop formed by the two a. c. windings contains only even components.
5. The emf, due to the cores but referring to the circuit through the a. c. source, contains only odd components.
6. The emf, due to the core, in the circuit through the d. c. source contains only even components.

These rules refer to quasi-stationary conditions, i. e. steady state with constant d. c. voltage U_m and an a. c. voltage U with constant value and frequency. Under transient conditions one may, for each instant, use the assumptions of quasi-stationary conditions but with a time derivative of all amplitudes and phase positions.

If subscripts o and e refer to odd and even components, and M is the resultant instantaneous mmf, then the following relations hold:

$$\begin{cases} i_{1o} = i_{2o} = \dfrac{i}{2} \\ i_{1e} = -\, i_{2e} \\ M_1 = N_m i_m + N i_{1o} + N i_{1e} = N_m i_m + \dfrac{Ni}{2} + N i_{1e} \\ M_2 = N_m i_m - N i_{2o} - N i_{2e} = N_m i_m - \dfrac{Ni}{2} + N i_{1e} \end{cases} \tag{1}$$

Under the assumption that the time derivative of Φ passes through zero only once per half cycle, which is true in all cases of practical interest, the maximum and minimum values of M thus follow the rules:

$$\begin{cases} \hat{M} = N_m \hat{\imath}_m + \dfrac{N\hat{\imath}}{2} + N\hat{\imath}_e \\ \check{M} = N_m \hat{\imath}_m - \dfrac{N\hat{\imath}}{2} + N\hat{\imath}_e \end{cases} \tag{2}$$

which furnishes the important result:

$$\hat{M} - \check{M} = N\hat{\imath} \tag{3}$$

This means that the path in an M-Φ-diagram, followed during one a. c. cycle, has a projection on the M-axis which is determined only by the amplitude of the a. c. current. The corresponding projection on the Φ-axis is determined by the half-cycle mean value of the emf only.

In case of a *series transductor*, which is not dealt with here, the above rules 1—6 are still valid, yet with certain modifications which are quite obvious and which need not be repeated here. An important conclusion is, however, that under the assumptions earlier made regarding the core and winding losses being neglected the series case can be deduced directly from the parallel case, simply by using twice the value of a. c. voltage and half the value of a. c. current. The following treatment may consequently in principle be understood to comprise both cases.

II.2 Simplified treatment of the a. c. circuit

In order to find an explanation, in principle, of the processes in a transductor with capacitor and resistor in series and being fed from an a. c. source of sinusoidal voltage, the diagram in fig. 1 a is used. The voltage U_L is measured across the a. c. winding of the transductor, which is supposed to have negligible losses. Only the fundamental components of current and voltages are taken into consideration. This means a very great approximation, which is, however, justified by the aim of the present step of the investigation, which is purely qualitative.

The phasor diagram of the circuit quantities will be in accordance with the figures 1 b and 1 c, referring to the two cases of U_L exceeding or being less than $\dfrac{I}{\omega C}$. In both cases the equations (4) are valid:

$$\begin{cases} U_L^2 + Z^2 I^2 - 2\, U_L\, XI = U^2 \\ Z^2 = R^2 + \dfrac{1}{\omega^2 C^2} = R^2 + X^2 \end{cases} \tag{4}$$

This means an ellipse as shown by fig. 2.

For given supply voltage U and different values of the resistance R the curves in fig. 2 are obtained. Fig. 3 a shows the straight lines

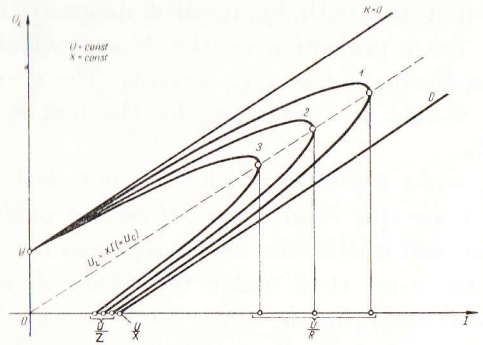

Fig. 2. Load characteristics for constant voltage U and variable resistance R.

corresponding to $R = 0$ for different values of U, while fig. 3 b illustrates the ellipses given by constant $R \neq 0$ and different U, the latter denoted by the figures 1, 2 and 3.

Next step will be to combine the curves shown by the figures 2—3, which are called *load characteristics*, with the magnetization curve of the transductor. At first, however, the d. c. excitation of the transductor is omitted, the voltage U_L thus referring to the terminals of an ordinary reactor with iron core. If the coordinates of the load characteristics denote effective values of current and voltage, the magnetization curve, as shown in the figures 4 and 5,

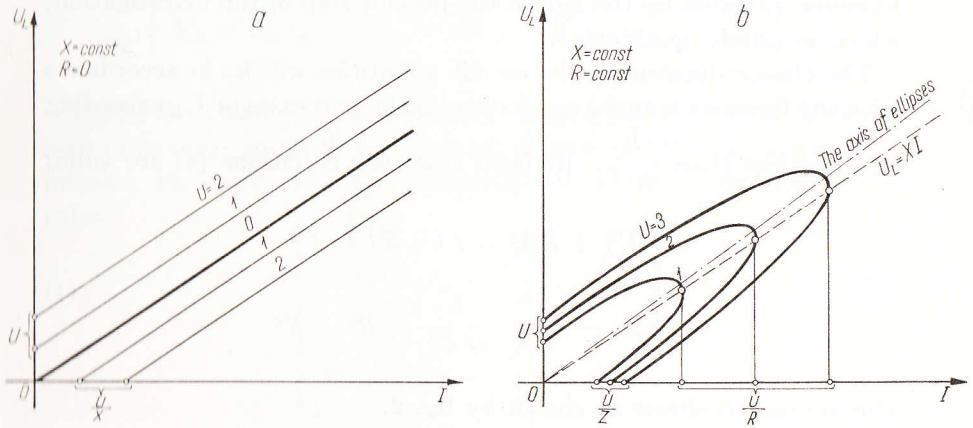

a. $R = 0$ b. $R \neq 0$

Fig. 3. Graph showing load characteristic of external a. c. circuit.

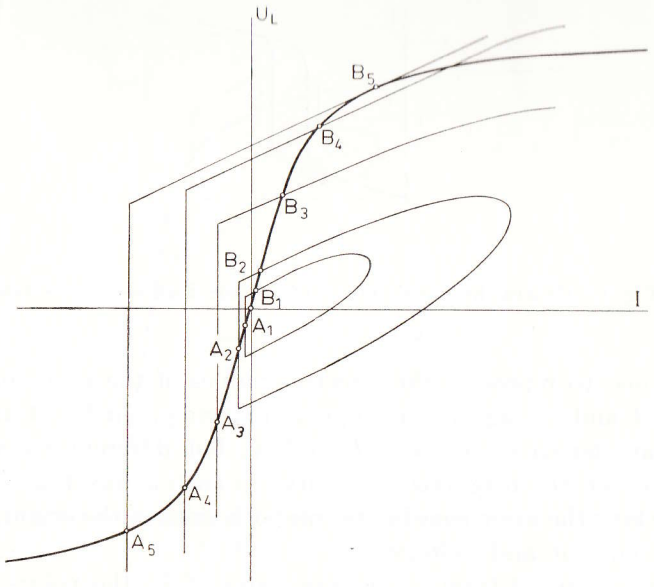

Fig. 4. Load characteristic superimposed on magnetization curve of reactor without d. c. excitation. Increasing voltage U.

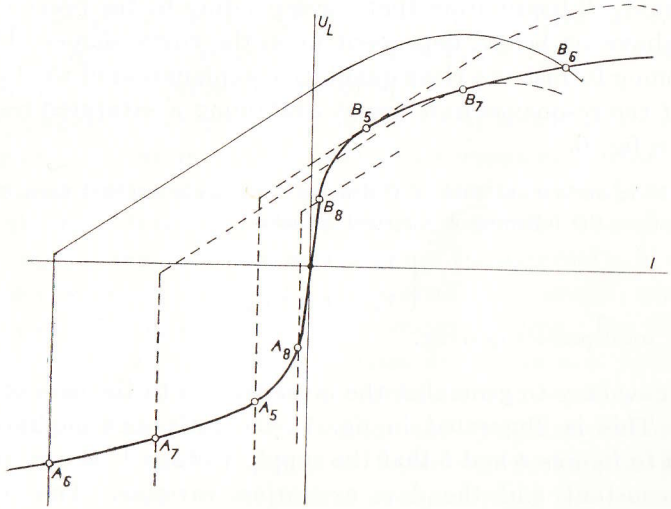

Fig. 5. Load characteristic superimposed on magnetization curve of reactor without d. c. excitation. Decreasing voltage U.

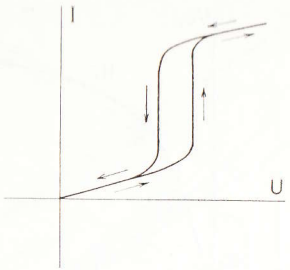

Fig. 6. General hysteresis effect of reactor with capacitive load.

is supposed to represent the effective values of the fundamentals of current I and voltage U_L at supply frequency. In fig. 4 and 5 the load characteristics for given R and X, but different values of U, are placed on the magnetization curve in such a way that the intersections give the same coordinates on both sides of the origin, relating to both current and voltage.

Starting in fig. 4 from a very low value of U, the points of intersection $A_1 B_1$ are obtained. Increasing U means the points $A_2 B_2$, $A_3 B_3$ and finally $A_5 B_5$, where the curves are tangents to each other. Raising U still more makes the points of intersection make a sudden jump to $A_6 B_6$ as shown in fig. 5. If U is now varied towards lower values the jump occurs at the points $A_7 B_7$, that means at a value considerably different from that corresponding to the previous jump, either above or below, dependent upon the curve shapes. This way of reasoning furnishes a clear qualitative explanation of the hysteresis effect of the resonance in a circuit containing a saturated reactor, as shown in fig. 6.

Note. It is understood that if V denotes the straight vertical part, of a curve in fig. 5, then the following is supposed to hold:

$$\begin{cases} V_6 = V_5 + \varepsilon \\ V_6 > V_7 > V_8 \end{cases}$$

ε being a small positive quantity.

It is now easy to generalize the investigation to the case of a *transductor*. This is illustrated in fig. 7, yet with such modification in relation to figures 4 and 5 that the supply voltage U is now supposed to be constant and the d. c. excitation variable. The fulldrawn curves 1, 2, 3 correspond to increasing excitation current I_m, while the dotted curve 4 shows the situation on the way down. Jumps

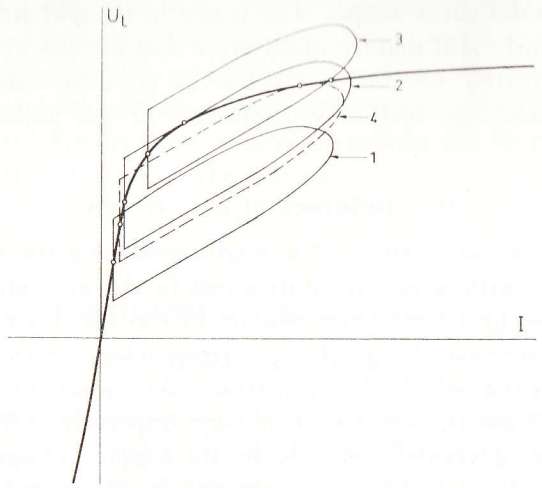

Fig. 7. Load characteristic superimposed on magnetization curve of transductor with variable d. c. excitation.

with hysteresis occur also in this case, just as in the case of the pure reactor. Obviously the variation could be done also by means of the supply voltage U or by both U and I_m.

It should be noticed that in fig. 7 the horizontal distance between the points of intersection belonging to the same position of the load characteristic are a measure of the a. c. current irrespective of the excitation current I_m relating to that position. This follows from equation (3) in the preceding paragraph.

If the magnetization curve is understood to be the static curve of the magnetic circuit it can be drawn to correspond to the current and terminal voltage in a totally general manner, even if the distortion of the time functions are taken into account. The abscissa is then the sum of the instantaneous values of the external a. c. current, twice the even components of the internal a. c. current, and twice the d. c. current referred to the same number of turns. The difference of the maximum and minimum abscissa during an a. c. cycle is the peak value of the a. c. current, as explained above. The difference of the maximum ordinate measures the half cycle mean value of the terminal voltage. It thus seems as if the constructions in fig. 4, 5 and 7 could be made quite general irrespective of the curve shape, which is always distorted due to the saturation. This is, however, not true, as the load characteristic has no exact meaning in the case

of non-sinusoidal curve-shape. The trains of thought followed above are consequently still mainly qualitative and involve an approximation, although they are very useful for the physical understanding of the phenomena. See further a discussion on this matter in section IV.3.

II.3 Influence of d. c. circuit

From the comments to fig. 7 it might seem as if the conditions in a transductor with a capacitor in series in the a. c. circuit are the same as those in an ordinary reactor in the same connection, i. e. involve two regions of operation, corresponding to the figures 1 b and 1 c, between which the transition takes place by jumps with hysteresis. There is, however, one very important difference. The d. c. circuit is governed not only by its supply voltage and its resistance but also by the emf originated by those variations of the total flux of the transductor which are due to the resultant effect of the a. c. and d. c. currents. The conditions are consequently very complicated. The differential equation of the d. c. circuit contains the time derivative of the zero-frequency component of the flux interlinked with that circuit, and certain influence is also exerted by the time harmonics of even order. The general procedure to study a certain state in the transductor is thus to solve the differential equation of the d. c. circuit, the state in the a. c. circuit being at each instant regarded as quasi-stationary. The result is that under certain conditions jumps occur when either U or I_m or both are varied, while under other conditions self sustained oscillations of low frequency are created, appearing in the electric circuits as amplitude modulations of great magnitude. Such a state means that the actual combination of supply voltage U and average excitation current is not compatible with steady state a. c. conditions but necessitates a periodical alternation between two steady states corresponding to two values of I_m, situated on both sides of the value $\frac{U_m}{R_m}$ determined by the d. c. supply voltage U_m and the d. c. circuit resistance R_m, and created by induction effect from the flux variations. This is the phenomenon which is the object of the present study.

The treatment of the modulation phenomenon can be made *either* by purely mathematical methods, expressing the magnetization curve by means of an analytic expression, *or* by graphical operations on

certain curves obtained from measurements. In the following the last mentioned method will be dealt with first and also illustrated by numerical examples. The mathematical method will then be exposed in principle and its consequences compared numerically with experimental results. Finally a series of oscillograms will be presented and discussed with reference to the theory.

III. Treatment on experimental basis

III.1 Definitions of symbols

As set forth in the preceding section the a. c. supply voltage U and the a. c. terminal voltage U_L of the transductor, as well as the current supplied from the power source to the a. c. circuit, are effective values, relating to a particular quasi-stationary state. In the preceding treatment of the a. c. circuit these quantities have been assumed to be sinusoidal, but as pointed out this is not true in practice. In the following the symbols U U_L and I still refer to effective values, the curve shape being arbitrary.

The symbols I_m and Φ_m, on the other hand, refer to mean values over an a. c. cycle in a particular quasi-stationary state. The voltage U_m is assumed to be a constant, but adjustable, quantity.

III.2 Classification of characteristic curves

In the preceding paragraphs the relationship between a. c. current and transductor terminal voltage, using supply voltage, resistance, and capacitive reactance as parameters, has been denoted as *load characteristic*. Another four characteristics will be useful for the treatment of experimental results and are defined in the following table, where for the sake of uniformity the above-mentioned curve is repeated.

1. *Load characteristic:*
   $U_L = U_L(I)$ $\quad$ U R X parameters

2. *Fundamental characteristic A:*
   $U_L = U_L(I)$ $\quad$ I_m parameter

3. *Fundamental characteristic B:*

$U_L = U_L(I)$ Φ_m parameter

4. *Control characteristics of transductor:*

a) $I = I(I_m)$ as plotted from 1 and 2

b) $I = I(\Phi_m)$ as plotted from 1 and 3
both with $U\ R\ X$ as parameters

5. *Magnetization characteristic of control winding:*

$\Phi_m = \Phi_m(I_m)$ as plotted from 4 a and 4 b.

The measurement of voltages and a. c. currents is, as said before, based on effective values, no consideration being paid to the distortion. This obviously means a certain approximation which must, however, be regarded as unavoidable. The flux is measured by means of fluxmeter, a method without objection, while the control current is measured by moving-coil ammeter, giving the arithmetical mean value.

III.3 Measurements on parallel transductor and plotting of curves

In order to clarify the general diagrams of connection the figures 8 a and 8 b illustrate the parallel and series transductor without self-excitation and with only one control winding. In the following the interest will be concentrated on the parallel tranductor, as has been pointed out earlier.

The diagram of connections for the determination of the characteristics of the transductor itself, without taking the load circuit into consideration, is shown in fig. 9. The instrument F is a fluxmeter; the other notations ought to be quite clear.

Conveniently the following two series of measurements are made:

In the first series the current I_m is kept constant at certain values, and for each such value the supply voltage is varied and the quantities U_L and I measured. U_L is plotted against I with I_m as a parameter. The result is the "fundamental characteristic A", the general shape of which is illustrated in fig. 10.

The next series aims at the "fundamental characteristic B", using the flux Φ_m as a parameter. Fluxmeter measurements are, however, not suitable for keeping a quantity constant, and it is therefore more

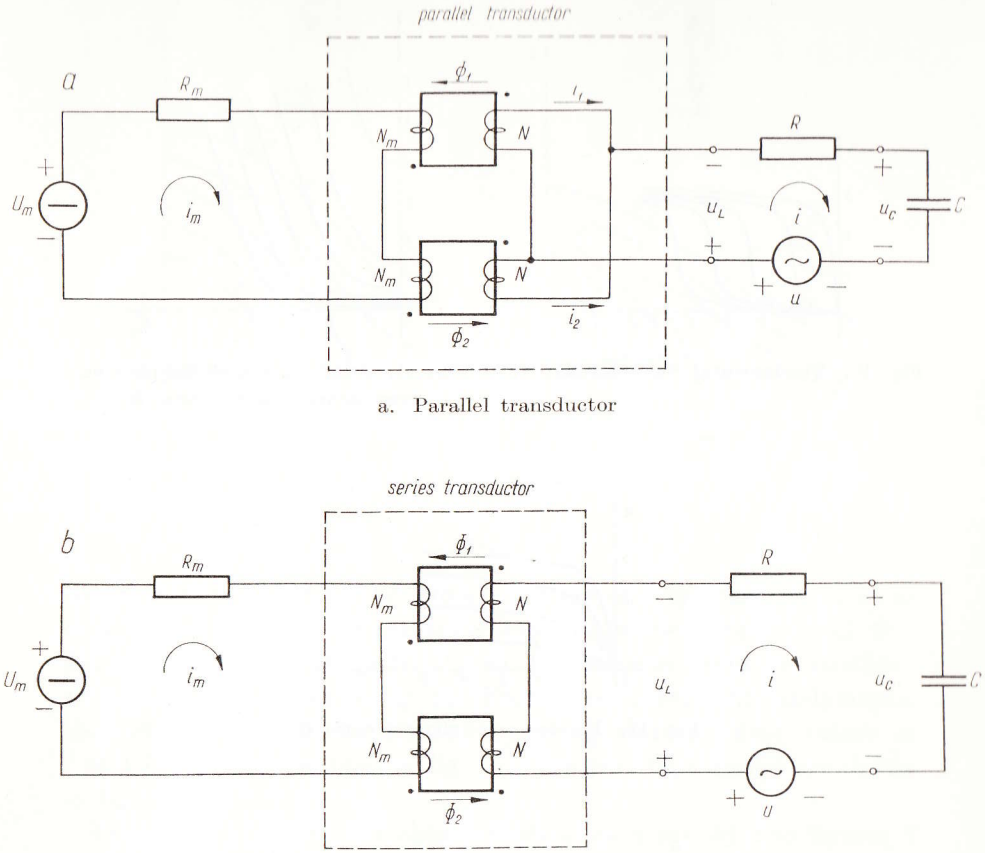

a. Parallel transductor

b. Series transductor

Fig. 8. Diagram of transductor without self-excitation.

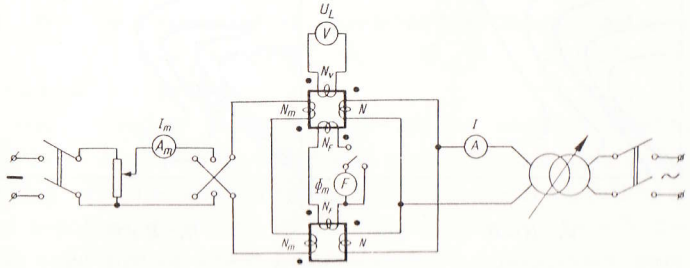

Fig. 9. Diagram of connections of test equipment for measurement of transductor data.

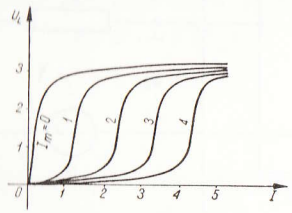

Fig. 10. Fundamental characteristic A.

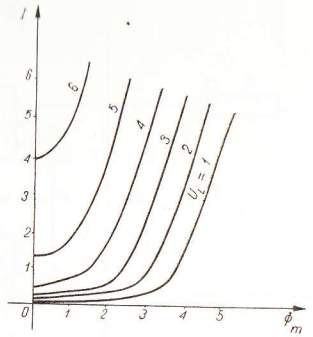

Fig. 11. Auxiliary curves for plotting fundamental characteristic B.

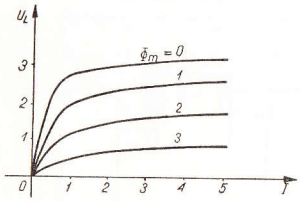

Fig. 12. Fundamental characteristic B.

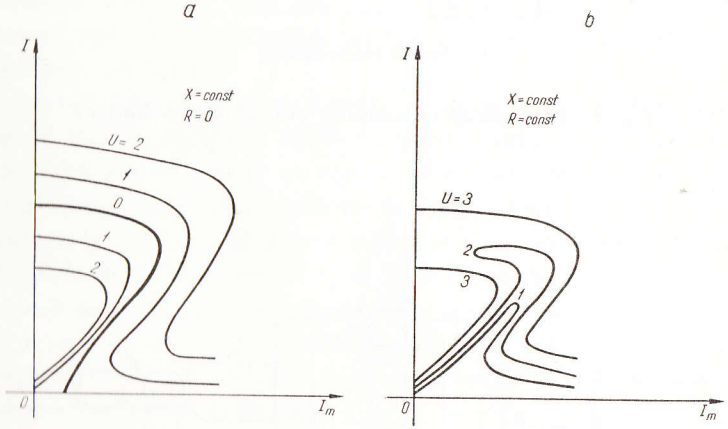

a. $R=0$ b. $R\neq 0$

Fig. 13. Graphs showing the function $I=I\,(I_m)$

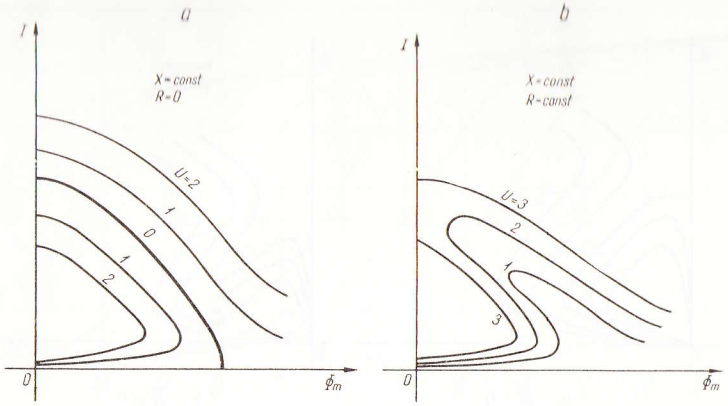

a. $R=0$ b. $R\neq 0$

Fig. 14. Graphs showing the function $I=I\,(\Phi_m)$

convenient to regulate the supply voltage and the current I_m so as to keep U_L constant at certain values, while measuring I and Φ_m. Plotting I against Φ_m with U_L as a parameter gives an auxiliary set of curves as shown in fig. 11. From these curves the fundamental characteristic B can be plotted by using corresponding values of I and U_L on vertical lines in fig. 11. The resultant curves are shown in fig. 12.

From now on the load characteristics, as given by the figures 2 and 3, can be introduced. Combining an actual load characteristic, related to certain values of U, R and X, with the curves in fig. 10, the relation $I = I\,(I_m)$ is obtained. The result is illustrated in the figures 13 a and 13 b. The same operation on fig. 12 gives the relation $I = I\,(\Phi_m)$ and is shown in the figures 14 a and 14 b. Finally, a combination of the figures 13 and 14, i. e. graphical elimination of the current I from these curves, furnishes the "magnetization characteristic of the control winding", $\Phi_m = \Phi_m\,(I_m)$, of the type shown in the figures 15 a and 15 b.

The magnetization characteristics of the control winding thus obtained have a surprising shape and constitute a rather complicated relationship. Peculiarities of these curves are the intervals of negative slope or *negative inductance of the control circuit*. As will be shown later the existence of these intervals play an important part in the creation of self-sustained modulations.

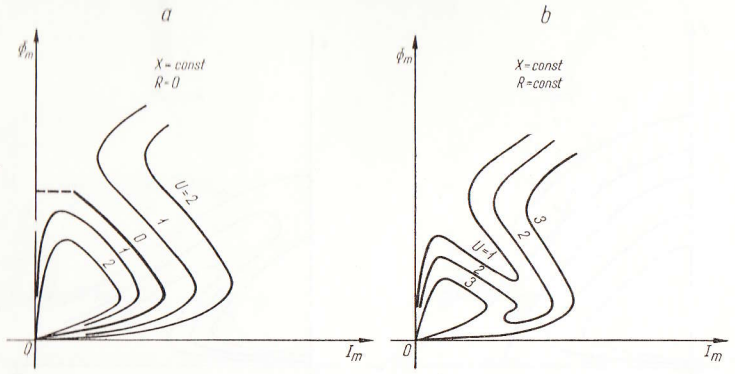

a. $R=0$ b. $R\neq 0$

Fig. 15. Graphs showing the magnetization characteristics of the control winding, $\Phi_m = \Phi_m(I_m)$.

Before entering into the study of the background of the modulations it might be of interest to quote some figures from measurements on an actual transductor.

The transductor used for the experiments is characterized by the data $N_m = 900$; $N = 860$; $f = 50$ Hz, and by the normal magnetization characteristic of each core as given in fig. 16. For the load

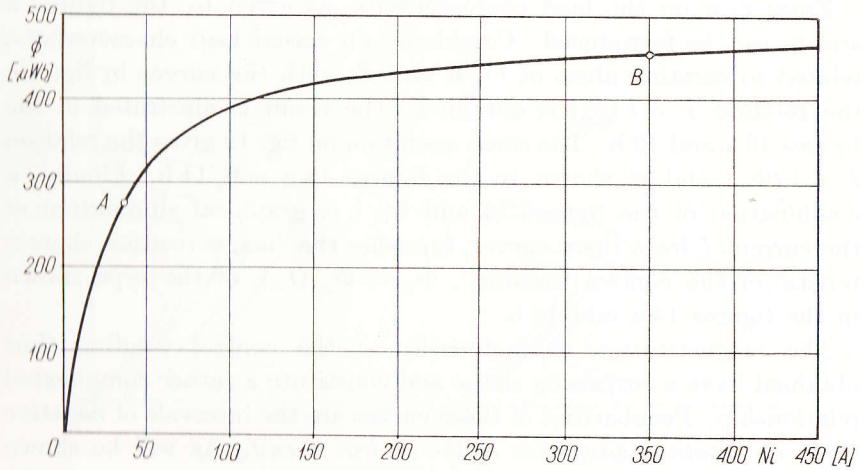

Fig. 16. Normal magnetization characteristic of transductor used for experimental investigations.

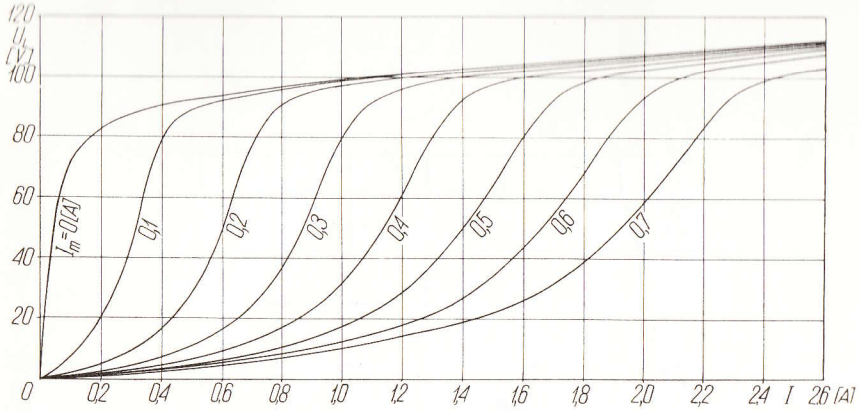

Fig. 17. Measured fundamental characteristic A.

circuit a series capacitance $C = 60\,\mu F$ has been used, corresponding to $X = 53{,}1\,\Omega$. For the load resistance the values were $R = 0$ and $R = 10{,}1\,\Omega$. The load characteristics used in the graphical procedures were based on the values $U = 0$, 10 and 20 V and $U = 15$, 20 and 25 V, for the two respective values of R.

The results of the measurements and the plotted curves are illustrated by the figures 17—24, the following correspondence being established between these figures and the general figures referred to in the above:

Fig. 10	fig. 17, 20 a, 20 b
» 11	» 18
» 12	» 19, 21 a, 21 b
» 13	» 22 a, 22 b
» 14	» 23 a, 23 b
» 15	» 24 a, 24 b

The figures 20 a, 20 b, 21 a, 21 b illustrate the combination of fundamental characteristic and load characteristic.

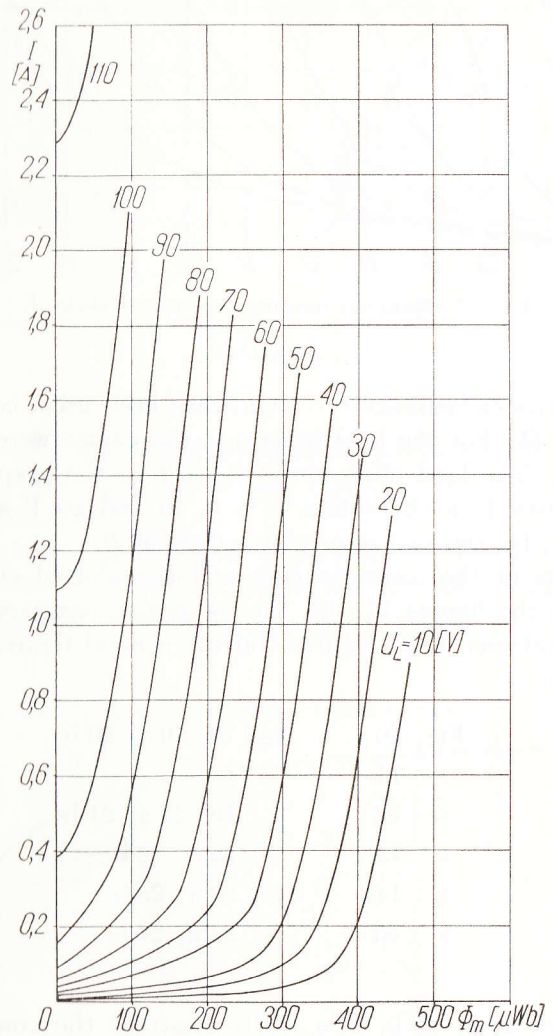

Fig. 18. Measured auxiliary curves for fundamental characteristic B.

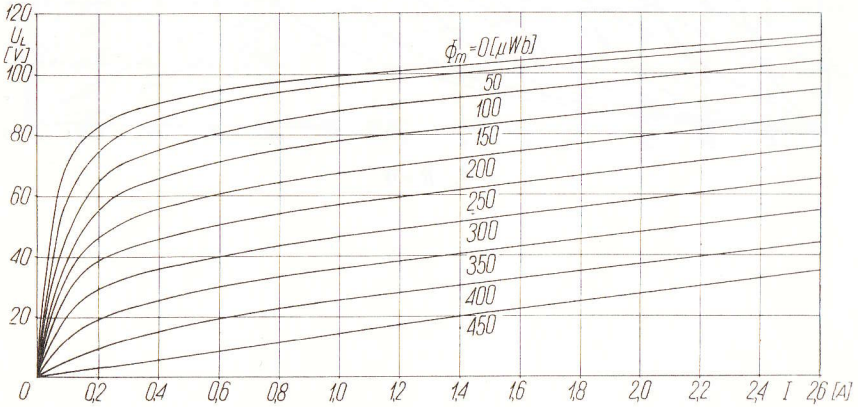

Fig. 19. Fundamental characteristic B obtained from measurements.

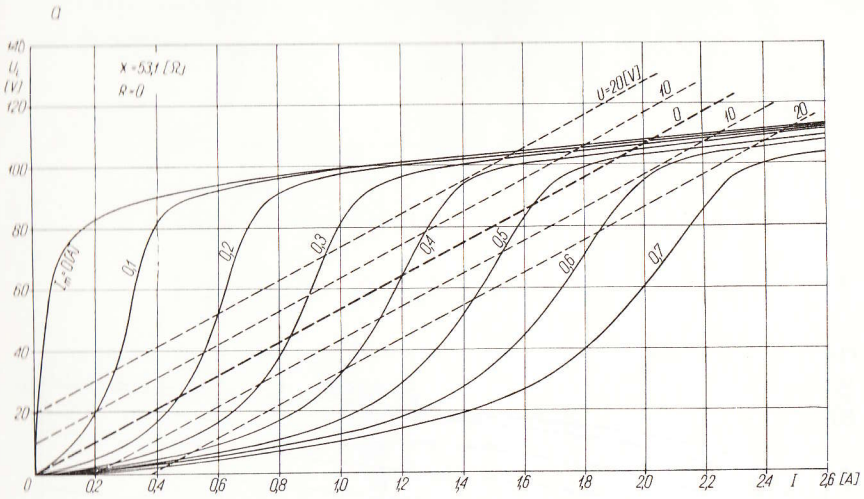

a. $R=0$

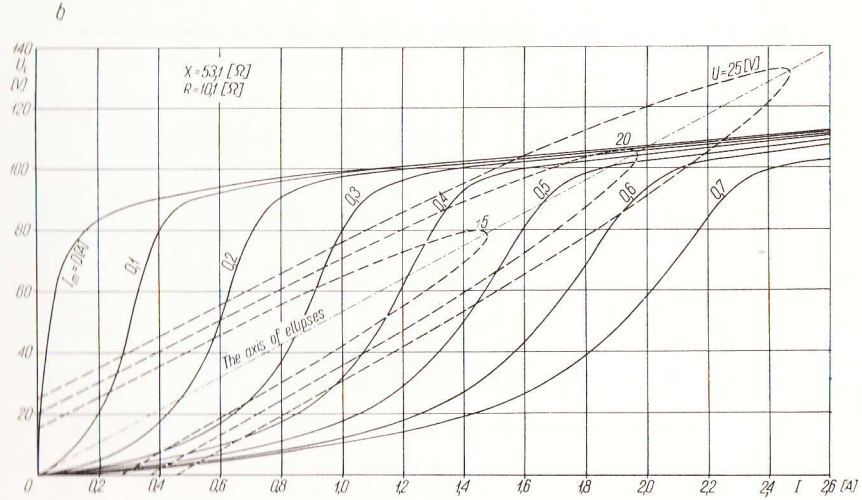

b. $R\neq 0$

Fig. 20. Combination of measured fundamental characteristic A and load characteristics

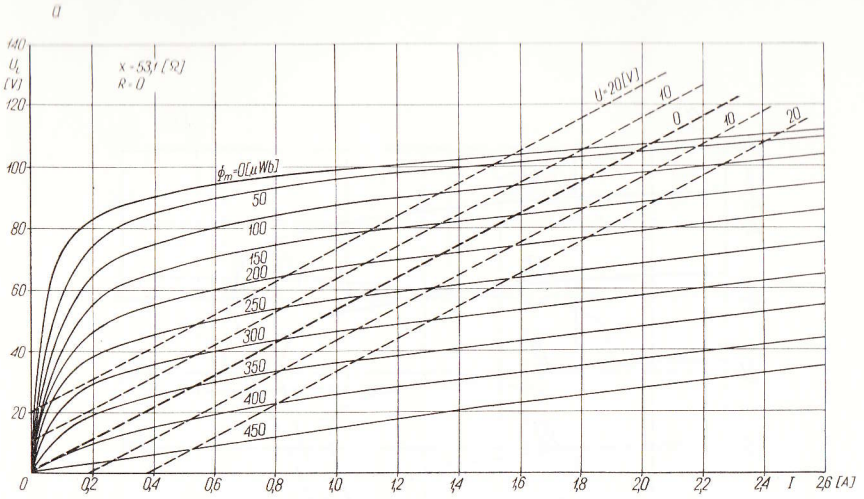

a. $R=0$

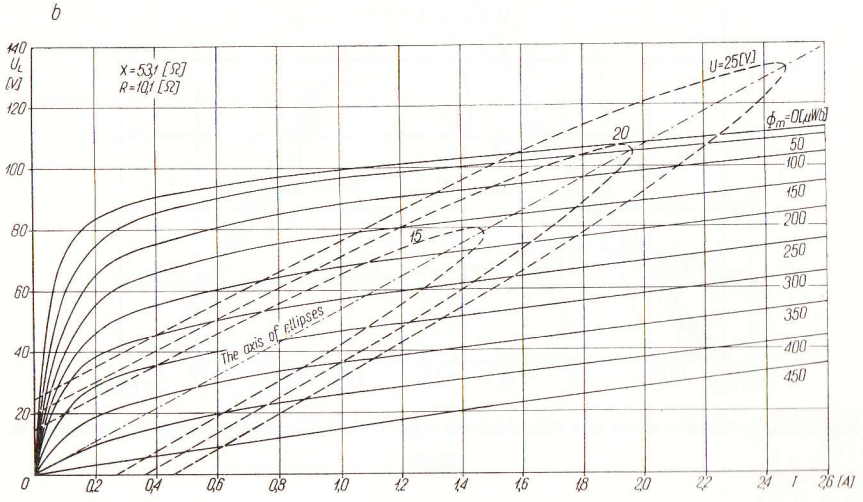

b. $R\neq 0$

Fig. 21. Combination of measured fundamental characteristic B and load characteristics

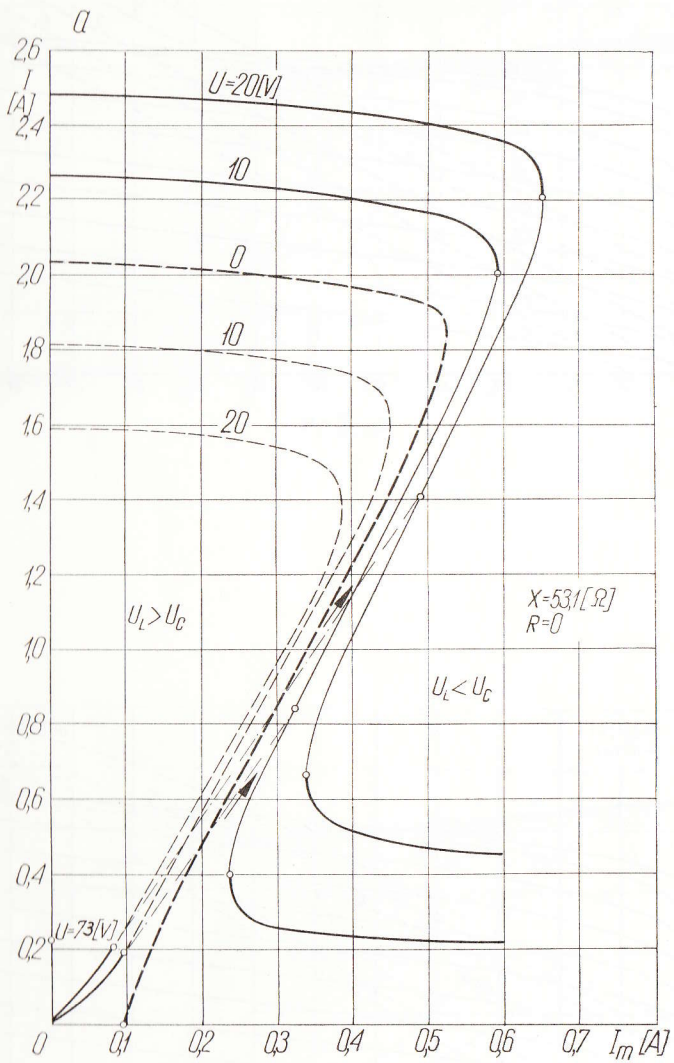

Fig. 22 a. Graph showing the function $I=I\,(I_m)$, obtained from measurements.
$R=0$

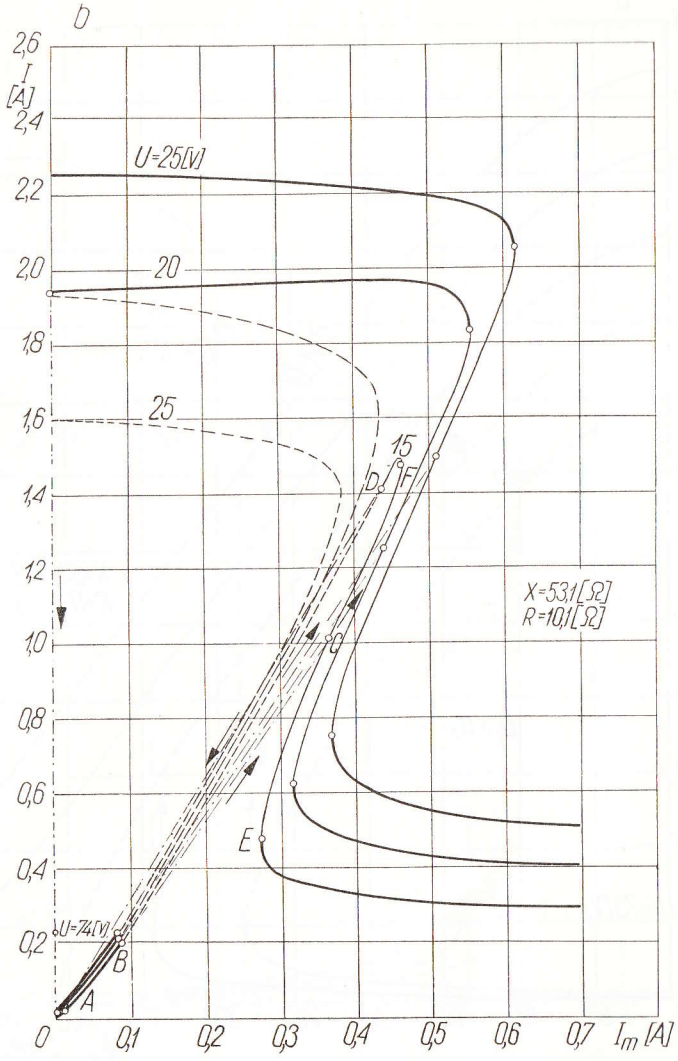

Fig. 22 b. Graph showing the function $I=I\,(I_m)$, obtained from measurements.
$R\neq 0$

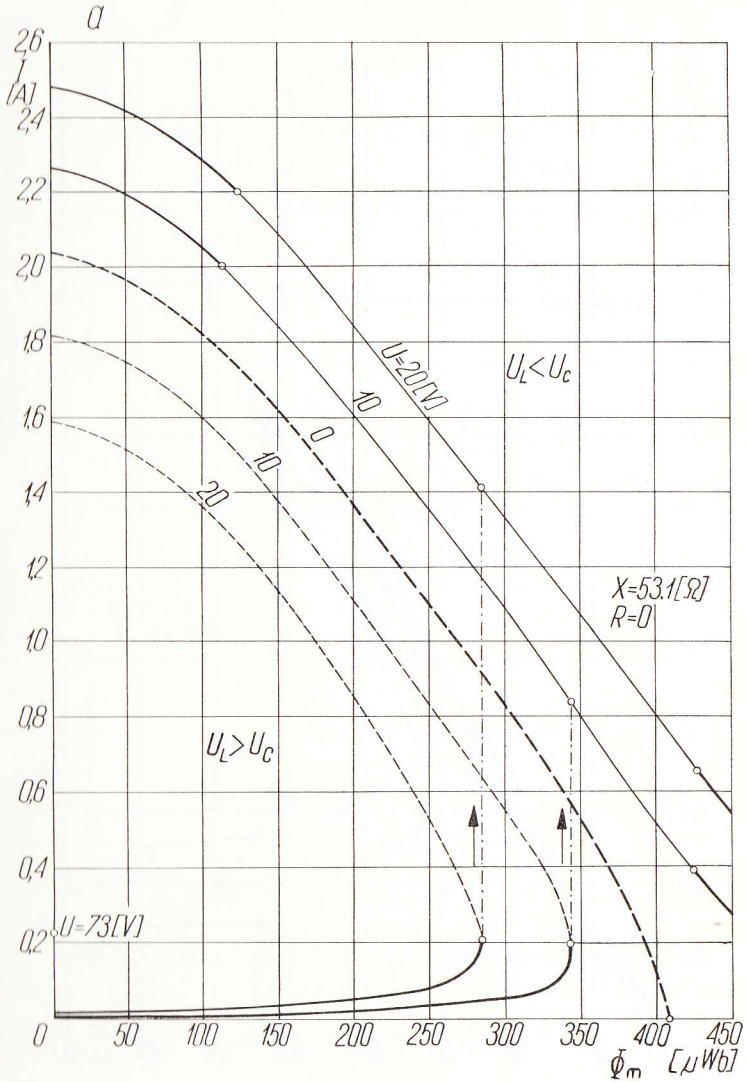

Fig. 23 a. Graph showing the function $I=I(\Phi_m)$, obtained from measurements.
$R=0$

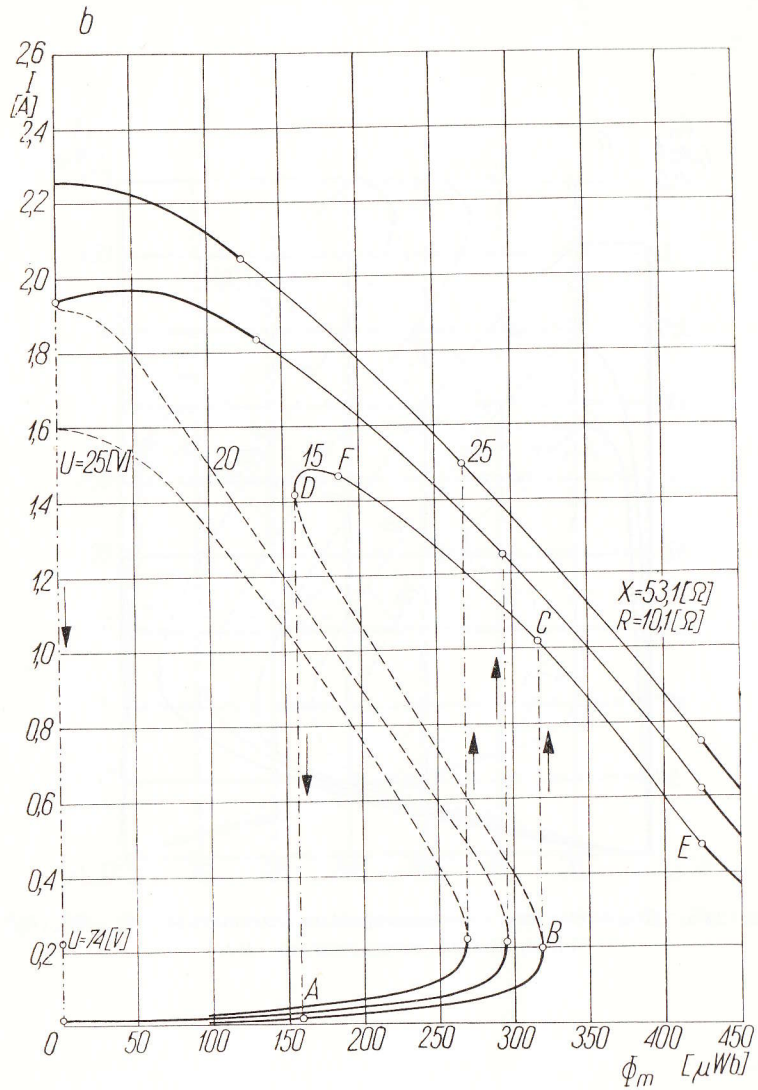

Fig. 23 b. Graph showing the function $I=I(\Phi_m)$, obtained from measurements.
$R\neq 0$

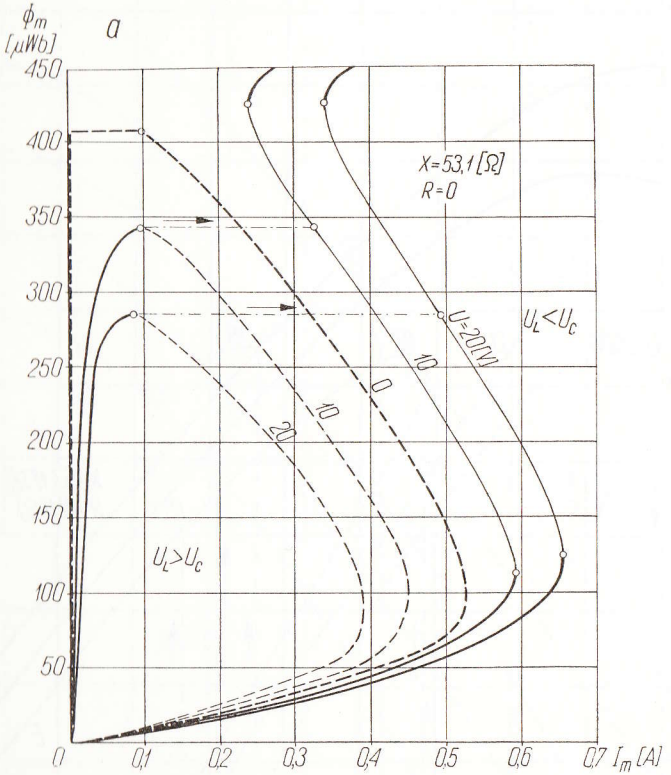

Fig. 24 a. Graph showing the magnetization characteristic, $\Phi_m=\Phi_m(I_m)$, obtained from measurements. $R=0$

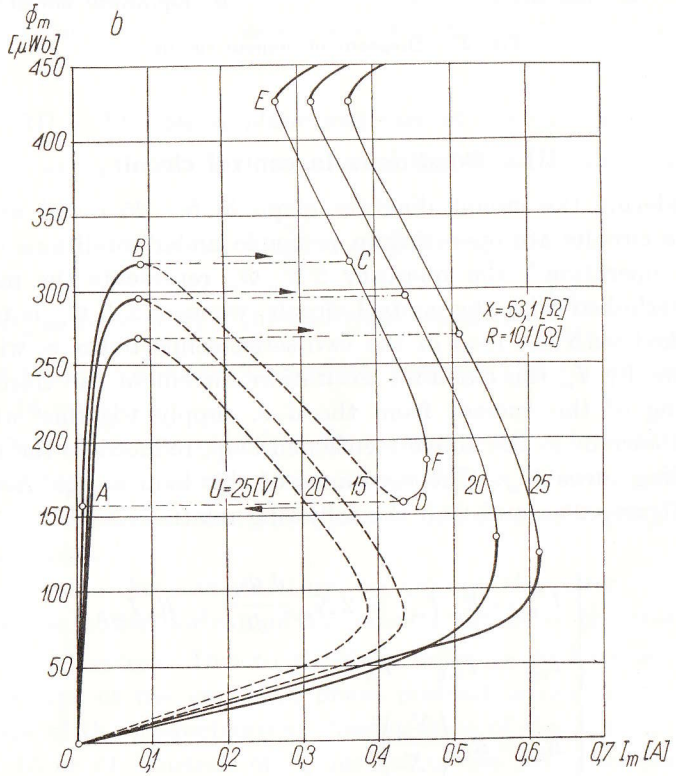

Fig. 24 b. Graph showing the magnetization characteristic, $\Phi_m=\Phi_m(I_m)$, obtained from measurements. $R\neq 0$

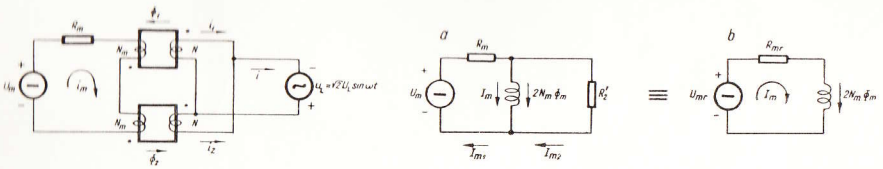

a. Real circuit b. Equivalent circuit

Fig. 25. Diagram of control circuit.

III.4 Conditions in control circuit

Considering the circuit diagram given in fig. 25 a and assuming that the circuits are operating in principle under conditions of "free current operation", the quantity $2\,N_m\,\Phi_m$ represents the magnetic flux interlinked with the control circuit, whereas $2\,N\,\Phi_m$ is the flux interlinked with the loop of the two series-connected a. c. windings.

Denote by I_m the resultant excitation current of the transductor consisting of the current from the d. c. supply together with the induced current in the above-mentioned loop, reduced to the number of winding turns N_m. The resistance of this loop is R_2. According to the figures 25 a and 25 b the following relations hold:

$$\begin{cases} U_m - R_m\,I_{m1} = 2\,N_m\dfrac{d\,\Phi_m}{dt} = R_2'\,I_{m2} \\ I_{m1} - I_{m2} = I_m \\ R_2' = R_2\left(\dfrac{N_m}{N}\right)^2 \end{cases} \tag{5}$$

which gives:

$$U_{mr} = R_{mr}\,I_m + 2\,N_m\frac{d\,\Phi_m}{dt} \tag{6}$$

where:

$$\begin{cases} U_{mr} = \dfrac{R_2'}{R_m + R_2'}\,U_m = \varrho\,U_m \\ R_{mr} = \dfrac{R_2'}{R_m + R_2'}\,R_m = \varrho\,R_m \end{cases} \tag{7}$$

In the previous paragraphs the current I dealt with has been understood as the a. c. current outside the closed loop formed by the transductor a. c. windings. The differential equation (6) of the control circuit contains the circulation current in the loop and thus completes the set of relations necessary for solving the problem of the processes in the transductor, when connected to the a. c. and d. c. sources and having the impedance elements R and X in series on the a. c. side.

III.5 The phase-plane analysis of control circuit

The equation (6) of the control circuit can be rewritten in the form:

$$\dot{\Phi}_m = -\frac{R_{mr}}{2\,N_m}\,I_m\,(\Phi_m) + \frac{U_{mr}}{2\,N_m} \tag{8}$$

where $\dot{\Phi}_m$ is the symbol of the first time derivative $\dfrac{d\,\Phi_m}{dt}$, and $I_m\,(\Phi_m)$ denotes that I_m is a function of Φ_m according to the curves in the figures 15 or 24.

The relation between the first time derivative of a function and the function itself, i. e. the expression $\dot{\Phi}_m\,(\Phi_m)$, is known as the *phase portrait* of a system, and the plane of coordinates $\Phi_m\,\dot{\Phi}_m$ is called the *phase-plane*.

According to this nomenclature, eq. (8) and the curves referred to describe the phase portrait of the control circuit of the transductor under consideration. Due to the linear relation (8) between $\dot{\Phi}_m$ and I_m the shape of the graphical phase portrait is exactly conform to the shape of the magnetization characteristic of the control winding, figures 15 or 24. Instead of I_m one has to use the expression in the right hand side of eq. (8), giving the multiplication by a negative factor and the addition of a positive term dependent on U_{mr}.

In fig. 26 are presented graphs of the phase portraits relating to the three most typical shapes of magnetization characteristics, and for some significant values of the transformed control voltage U_{mr}. Practically, these graphs take into account all possible conditions of the transductor operation when the capacitive load is predominating.

Each one of the three columns (a, b, c) in fig. 26 corresponds to one single combination of $U\,R\,X$, specifically relating to one case of fig. 15 a and two cases of fig. 15 b. Within each column the cases differ by the value of $\dfrac{U_m}{R_m}$.

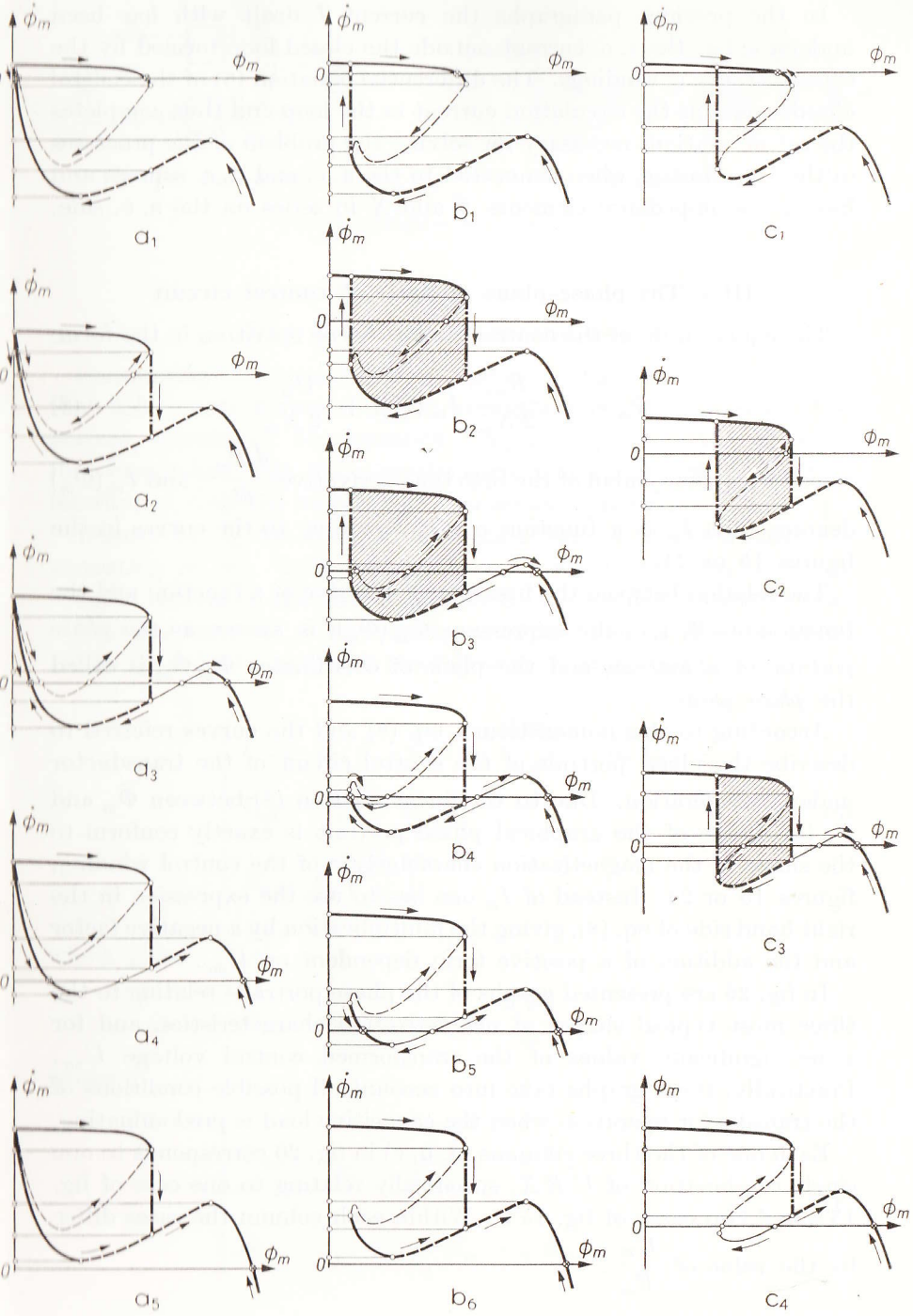

Fig. 26. Graphs of phase portraits.

The notations used in fig. 26 have the following meaning:

——————— segments of the phase path, being the locus of all possible points of stable equilibrium.

– – – – – – – – a segment of the phase path, along which, for given value of control voltage, the working point can move during a transient state, including modulations.

——————— a segment of the phase path which, for given value of control voltage, can not be attained by the working point, neither during steady state nor during a transient.

– – – – – – – – a segment of the phase path, which is excluded from being attained by the working point for all values of control voltage and under all conditions.

— · — · — · — a segment of a *jump* in phase path

⊗ a point of *stable equilibrium*

//////// an area bounded by a *stable limit cycle*

All the properties of the circuits indicated on the graphs of fig. 26 are the logical consequences of the two self-evident rules:

1. Positive $\dot{\Phi}_m$ corresponds to a rising value of Φ_m, and vice versa.
2. The time intervals of the jumps, when the working point has been forced to leave the phase path, can be regarded as zero.

Thus, according to the same graphs, there are in steady state the following possible modes of operation of the transductor under consideration:

1. For all initial conditions there is one and only one stable point, cases 26 $a_2\ a_5\ b_1\ b_6\ c_1\ c_4$.
2. There are two stable points depending upon the initial conditions, cases 26 $a_1\ a_3\ a_4\ b_4\ b_5$.
3. For some initial conditions there is a stable point, for the others a *stable limit cycle*, cases 26 $b_3\ c_3$.
4. For all initial conditions there is only a *stable limit cycle*, cases 26 $b_2\ c_2$.

In other words, for some values of the parameters, due to the presence of a stable limit cycle in the phase portrait of the system there must occur *stable oscillations* of the flux Φ_m and consequently of the excitation current I_m as well as of the a. c. current I and the voltage across the various elements of the a. c. circuit. These oscillations can be said to be of the so called *relaxation type*. It must be noted that the oscillations on the a. c. side do not have the character of subharmonics but are actually amplitude modulations, just as mentioned in the introduction. The origin of the phenomenon of self-sustained modulations in transductor circuits with capacitor in the a. c. circuit is thus qualitatively explained.

III.6 Conditions for occurrence of self-sustained modulations

From fig. 26 it is obvious that a stable point always corresponds to the conditions $\dot{\Phi}_m = 0$ and $\frac{d\dot{\Phi}_m}{d\Phi_m} < 0$. The first condition is self-evident by definition, and the second follows from the rule that positive derivative with respect to time means rising flux, and vice versa. All stable points are consequently situated at the intersection of a sloping branch of the phase portrait with the abscissa axis. In dependence of the *shape* of the phase portrait (or of the Φ_m-I_m-curve according to fig. 15) and of the actual value of the stationary excitation current $\frac{U_m}{R_m}$, there exists or does not exist a point of intersection of the said type. If such a point does not exist (fig. 26 b_2 c_2) oscillations occur for any initial state. If one or more stable points exist and can be attained from any initial state, then no oscillation takes place. Finally, there are cases (fig. 26 b_3 c_3) when a stable point exists but can be attained only from a certain range of initial states. In this case oscillations may or may not occur.

For the sake of clarity it should be repeated that the instantaneous value i_m of the magnetization current oscillates around its mean value I_m during an a. c. cycle, the value I_m referring to a given quasi-stationary state. During a transient process I_m varies, and during a modulation cycle it oscillates with modulation frequency around its own mean value $\frac{U_m}{R_m}$.

For each shape of the phase portrait, i. e. for each combination of U R and X, where the condition for self-sustained modulations is fulfilled, the total range of stationary-excitation current $\frac{U_m}{R_m}$ comprises a certain *range of modulations*, within which modulations are possible. In such cases where for certain values of $\frac{U_m}{R_m}$ a stable point exists but is not attainable from any initial state, the range of modulations may be subdivided into one *sub-range of absolute modulations*, where modulations necessarily occur, and one *sub-range of conditional modulations*, where modulations do or do not occur, dependent upon the initial conditions. Examples are shown in the figures 27 a and 27 b, related to the second and third column in fig. 26.

The general problem to formulate a criterium, involving characteristical data of the transductor and the circuits, for the possibility of self-sustained modulations seems to be very difficult or at least very complicated. One feature is, however, interesting to note. The theoretical case $R = 0$, furnishing a load characteristic which consists of two traight lines, makes the phase portrait take a shape which permits stable points starting from any initial state, that is prevents modulations. In practical cases a certain resistance always exists, even if not deliberately introduced in the circuit, but a non-negligible value of this resistance is a necessary condition for the occurrence of modulations. On the other hand, a very high resistance prevents such modulations.

Another conclusion, which arises from a comparison of the figures 15 and 26, is that, for given value of the resistance R, the modulations will be possible only for a certain range of the a. c. voltage U. As can be easily shown, the upper limit of this voltage is determined, with some approximation, by the condition that the load characteristic is tangent to the fundamental characteristic corresponding to the parameter $I_m = 0$.

a

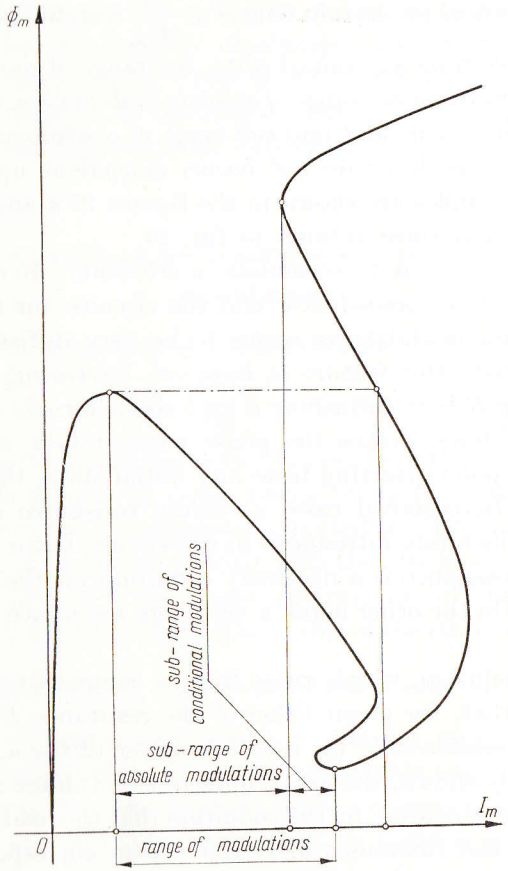

Fig. 27 a. Graph illustrating ranges of modulation. Second column in fig. 26.

b

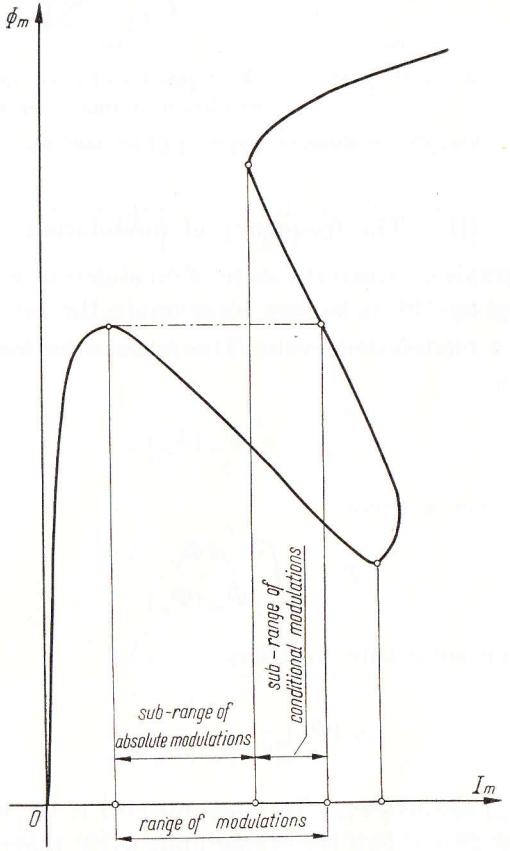

Fig. 27 b. Graph illustrating ranges of modulation. Third column in fig. 26.

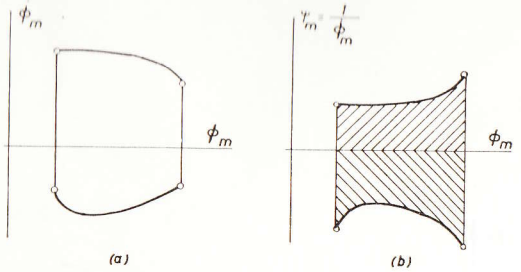

a. Real cycle. b. Cycle transformed for calculation of time intervals.

Fig. 28. Modulation cycle in phase portrait

III.7 The frequency of modulation

When the graph of a certain state of modulation is known in the shape given by fig. 26, it is easy to compute the total period T, in seconds, of the modulation cycle. The relation between $\dot{\Phi}_m$ and Φ_m can be written:

$$\frac{d\,\Phi_m}{dt} = \dot{\Phi}_m\,(\Phi_m) \tag{9}$$

or integrated over a cycle:

$$T = \int \frac{d\,\Phi_m}{\dot{\Phi}_m\,(\Phi_m)} \tag{10}$$

Introduce the substitute function:

$$\psi\,(\Phi_m) = \frac{1}{\dot{\Phi}_m\,(\Phi_m)} \tag{11}$$

and plot $\psi\,(\Phi_m)$ against Φ_m. The integral (10) is the shaded area in fig. 28 b where 28 a shows the stable limit cycle taken from fig. 26.

The frequency of modulation is then expressed as:

$$f_m = \frac{1}{T} \tag{12}$$

It should be noticed that fig. 28 b also gives information regarding the time intervals of high respectively low values of I and I_m, the interval of high values being the area below the Φ_m-axis, and vice versa. This is understood from eq. (8).

IV. The analytical method

IV.1 Analytical representation of the magnetization curve

Among all those analytical expressions which have been used or proposed for approximating the magnetization curve of a core the following seems to be most suitable for the present purpose and will be used in this paragraph:

$$\Sigma\, Ni = \alpha \sinh \beta\, \Phi_m \tag{13}$$

where α and β are constants characteristic for the core.

The analytical treatment is considerably simplified by the use of dimensionless quantities which makes it possible to present all relations in a universal form. The dimensionless quantities are denoted by the usual symbols, yet with asterisks. The relations between dimensional and dimensionless quantities in the present case are as follows:

$$\begin{cases} U_L = \dfrac{\omega N}{\beta \sqrt{2}}\, U_L^* \\ I = \dfrac{\alpha}{N}\, I^* \\ I_m = \dfrac{\alpha}{N_m}\, I_m^* \\ \Phi_m = \dfrac{1}{\beta}\, \Phi_m^* \end{cases} \tag{14}$$

For a given iron core, the magnetization curve of which is known, the constants α and β are determined from assumed coincidence in two points, besides the origin. One point is suitably chosen somewhere below the knee and the other in the region of saturation. Denote these points by A and B, and the corresponding coordinates of the real curve by $(Ni)_A\,(\Phi_m)_A\,(Ni)_B\,(\Phi_m)_B$. The relations are then:

$$\begin{cases} (Ni)_A = \alpha \sinh \beta\,(\Phi_m)_A \\ (Ni)_B = \alpha \sinh \beta\,(\Phi_m)_B \end{cases} \tag{15}$$

Within the region of the points A and B we can approximate:

$$\sinh \beta \Phi_m \approx \frac{1}{2} e^{\beta \Phi_m} \tag{16}$$

Equations (15) thus become:

$$\begin{cases} \dfrac{(Ni)_B}{(Ni)_A} = e^{\beta [(\Phi_m)_B - (\Phi_m)_A]} \\ \\ \alpha = \dfrac{(Ni)_A}{\sinh \beta (\Phi_m)_A} \end{cases} \tag{17}$$

with the solution:

$$\begin{cases} \beta = \dfrac{\ln \dfrac{(Ni)_B}{(Ni)_A}}{(\Phi_m)_B - (\Phi_m)_A} \\ \\ \alpha = \dfrac{(Ni)_A}{\sinh \beta (\Phi_m)_A} \end{cases} \tag{18}$$

The transition from the universal curves to the curves for a given transductor is illustrated by the following example, referring to the transductor used for the experimental investigation, as mentioned earlier in section III.3. This transductor is characterized by the following data:

$$\begin{cases} N = 860 \\ N_m = 900 \\ \omega = 2\pi \cdot 50 = 314 \end{cases}$$

and by the magnetization curve shown in fig. 16.

From this curve the following points are taken:

$$\begin{cases} (Ni)_A = 35 \text{ A} \\ (\Phi_m)_A = 273 \cdot 10^{-6} \text{ Wb} \end{cases} \qquad \begin{cases} (Ni)_B = 350 \text{ A} \\ (\Phi_m)_B = 455 \cdot 10^{-6} \text{ Wb} \end{cases}$$

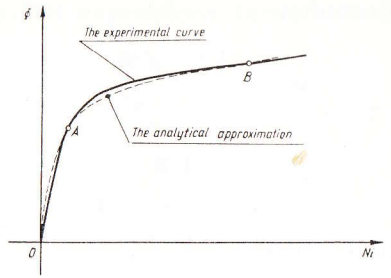

Fig. 29. Experimental and analytical magnetization curves.

Eq. (18) now gives:

$$\begin{cases} \beta = \dfrac{\ln 10}{(455 - 273) \cdot 10^{-6}} = 12{,}5 \cdot 10^3 \text{ Wb}^{-1} \\ \\ \alpha = \dfrac{35}{\sinh 3{,}42} = 2{,}29 \text{ A} \end{cases}$$

From eq. (14) is computed:

$$\begin{aligned} U_L &= 15{,}3\, U_L^* && \text{V} \\ I &= 2{,}66 \cdot 10^{-3}\, I^* && \text{A} \\ I_m &= 2{,}54 \cdot 10^{-3}\, I_m^* && \text{A} \\ \Phi_m &= 80 \cdot 10^{-6}\, \Phi_m^* && \text{Wb} \end{aligned}$$

A comparison between experimental and analytical curve is shown in fig. 29.

IV.2 Equations of universal fundamental characteristics

In this section a mathematical theory will be developed, referring to the transductor itself with a. c. voltage assumed sinusoidal, i. e. neglecting its harmonics. All quantities are expressed in the dimensionless form according to eq. (14), and the magnetization curve is represented by the expression (13). For the sake of simplicity the asterisks, denoting the dimensionless quantities, are left out.

Assuming the resistances and leakage reactances of the transductor as negligible the following equations are valid for the instantaneous values of the quantities relating to the two transductor elements.

For the electric circuits:

$$u_L = \frac{\sqrt{2}}{\omega}\frac{d\Phi_1}{dt}$$
$$u_L = -\frac{\sqrt{2}}{\omega}\frac{d\Phi_2}{dt} \tag{19}$$

For the magnetic circuits:

$$i_m + i_1 = \sinh \Phi_1$$
$$i_m - i_2 = \sinh \Phi_2 \tag{20}$$

Assume:

$$u_L = U_L \sqrt{2} \sin \omega t \tag{21}$$

Integration of eq. (19) by the aid of (21) then gives:

$$\Phi_1 = \Phi_m - \hat{\Phi} \cos \omega t$$
$$\Phi_2 = \Phi_m + \hat{\Phi} \cos \omega t \tag{22}$$

the flux amplitude $\hat{\Phi}$ being, in the dimensionless system, identical to the effective voltage U_L. Φ_m is so far an arbitrary constant.

In order to compute Φ_m it is practical to add eq. (20) and substitute from eq. (22). This furnishes:

$$2\, i_m + (i_1 - i_2) = \sinh [\Phi_m - \hat{\Phi} \cos \omega t] +$$
$$+ \sinh [\Phi_m + \hat{\Phi} \cos \omega t] = 2 \sinh \Phi_m \cosh [\hat{\Phi} \cos \omega t] \tag{23}$$

By instead subtracting eq. (20) the result is obtained:

$$i_1 + i_2 = i = \sinh [\Phi_m - \hat{\Phi}_m \cos \omega t] -$$
$$- \sinh [\Phi_m + \hat{\Phi} \cos \omega t] = -2 \cosh \Phi_m \sinh [\hat{\Phi} \cos \omega t] \tag{24}$$

Now, a Fourier expansion formula states that:

$$\begin{cases} e^{\hat{\Phi} \cos \omega t} = I_o(\hat{\Phi}) + 2 \sum_{n=1}^{\infty} I_n(\hat{\Phi}) \cos n\, \omega t \\ e^{-\hat{\Phi} \cos \omega t} = I_o(\hat{\Phi}) + 2 \sum_{n=1}^{\infty} (-1)^n I_n(\hat{\Phi}) \cos n\, \omega t \end{cases} \tag{25}$$

where I_n is the modified Bessel function of order n.

The use of these last expressions turns equations (23) and (24) into the form:

$$\begin{cases} 2\, i_m + (i_1 - i_2) = 2 \sinh \Phi_m [I_o(\hat{\Phi}) + 2\, I_2(\hat{\Phi}) \cos 2\, \omega t + \\ \qquad + 2\, I_4(\hat{\Phi}) \cos 4\, \omega t + \ldots .] \end{cases} \tag{26}$$

$$i = -4 \cosh \Phi_m [I_1(\hat{\Phi}) \cos \omega t + I_3(\hat{\Phi}) \cos 3\, \omega t + \ldots .] \tag{27}$$

In eq. (26) the constant term must be the same on both sides, consequently:

$$I'_m = I_o(\hat{\Phi}) \sinh \Phi_m \tag{28}$$

where, in order to avoid confusion with the symbol of modified Bessel function the notation I'_m is introduced for the mean value of the current on the d. c. side.

Eq. (28) gives:

$$\cosh \Phi_m = \sqrt{1 + \left(\frac{I'_m}{I_o(\hat{\Phi})}\right)^2} \tag{29}$$

and consequently the a. c. current i can be deduced from eq. (27):

$$i = -4 \sqrt{1 + \left(\frac{I'_m}{I_o(\hat{\Phi})}\right)^2} [I_1(\hat{\Phi}) \cos \omega t + I_3(\hat{\Phi}) \cos 3\, \omega t + \ldots] \tag{30}$$

The effective value of the fundamental of the a. c. current is thus:

$$I = 2\sqrt{2} \sqrt{1 + \left(\frac{I'_m}{I_o(\hat{\Phi})}\right)^2} I_1(\hat{\Phi}) \tag{31}$$

or after returning to the notation U_L and reintroducing the notation with asterisks:

$$I^* = 2\sqrt{2} \sqrt{1 + \left(\frac{I^*_m}{I_o(U^*_L)}\right)^2} I_1(U^*_L) \tag{32}$$

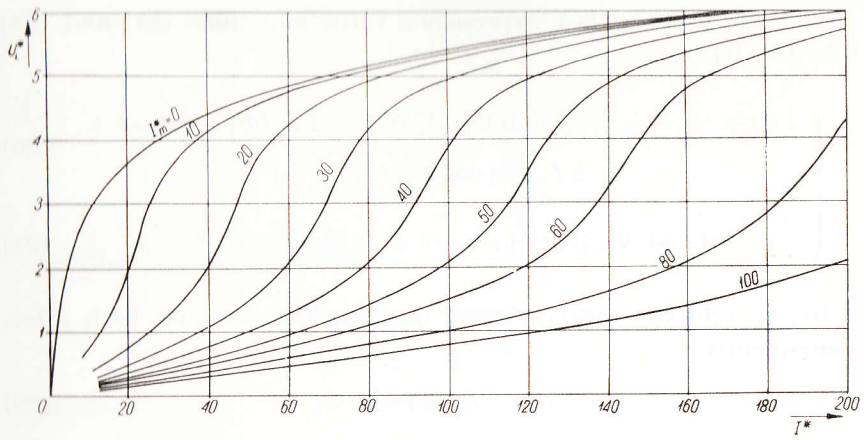

Fig. 30. Universal fundamental characteristic A.

Replacing the square root by its expression according to eq. (29) the following is obtained:

$$I^* = 2\sqrt{2}\,[\cosh \Phi_m^*]\, I_1\,(U_L^*) \tag{33}$$

The two equations (32) and (33) give the *universal fundamental characteristics A and B of the transductor.*

For constant parameters I_m^* and Φ_m^* they furnish the universal dimensionless correspondence to the curves earlier illustrated in the figures 17 and 19, and also correspond to the actual numerical experi-

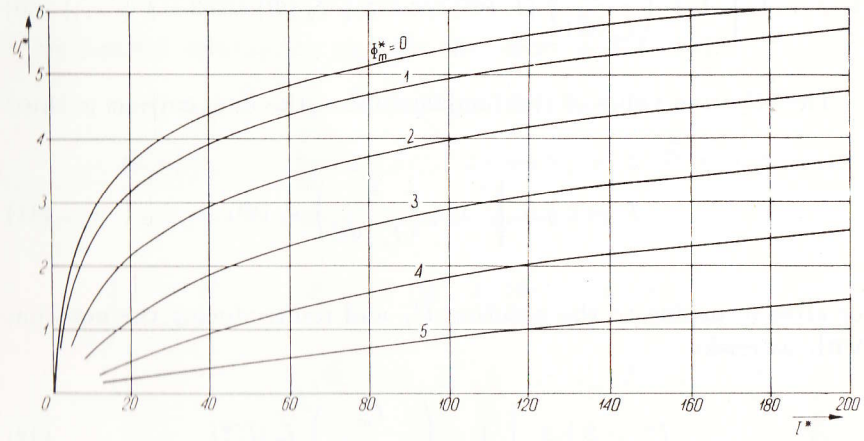

Fig. 31. Universal fundamental characteristic B.

mental curves shown in fig. 20 and 21. The universal curves according to eq. (32) and (33) are given in the figures 30 and 31. A comparison between fig. 20 and 21 on one side and fig. 30 and 31 on the other show very good similarity in general shape, and also good numerical agreement after introduction of the transition coefficients from eq. (14).

IV.3 Influence of harmonics

It is of interest to study the ratio of resultant effective value of the a. c. current to effective value of its fundamental. The former value can be written, according to eq. (30):

$$I_\Sigma^* = 2\sqrt{2}\,\sqrt{1 + \left(\frac{I_m^*}{I_o\,(U_L^*)}\right)^2}\,\sqrt{\sum_{n=1}^{\infty} [I_{2n-1}\,(U_L^*)]^2} \tag{34}$$

The ratio to be investigated is consequently:

$$k_e = \frac{I_\Sigma^*}{I^*} = \frac{1}{I_1\,(U_L^*)}\,\sqrt{\sum_{n=1}^{\infty} [I_{2n-1}\,(U_L^*)]^2} \tag{35}$$

A formula from the theory of Bessel functions states that:

$$\sum_{n=1}^{\infty} [I_{2n-1}\,(x)]^2 = \frac{1}{4}\,[I_o\,(2\,x) - 1] \tag{36}$$

which gives:

$$k_e = \frac{\sqrt{I_o\,(2\,U_L^*) - 1}}{2\,I_1\,(U_L^*)} \tag{37}$$

When estimating the order of magnitude of the errors introduced by replacing the real currents by their fundamentals, as has been done in the whole of the preceding approximate theory, it is, however, more adequate to study the ratio of peak values instead of effective values. This is due to the fact that the width of the region of magnetization curve covered during each a. c. cycle is determined by the peak value of the external a. c. current I, as is understood from eq. (3). According to eq. (30) the ratio of resultant peak value to peak value of fundamental is:

$$k_p = \frac{1}{I_1\,(U_L^*)} \sum_{n=1}^{\infty} [I_{2n-1}\,(U_L^*)] \tag{38}$$

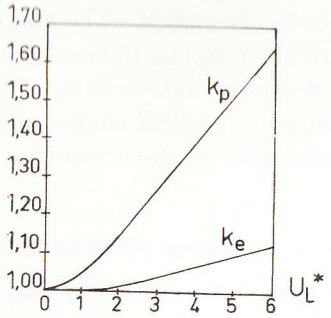

Fig. 32. Graph of quantities k_e and k_p showing influence of harmonics on effective and peak value of a. c. current.

In this case there does not seem to exist a general formula corresponding to that presented in eq. (37), but the ratio k_p can easily be computed from tables of functions, as the series in eq. (38) is rapidly convergent.

The graphs $k_e = k_e(U_L^*)$ and $k_p = k_p(U_L^*)$ are presented in fig. 32. They show that for high saturations the influence of harmonics is of the order of magnitude of 10 and 50 per cent relating to k_e and k_p respectively. This confirms the opinion that the theory presented in the paragraphs II—III involves a fairly rough approximation. The errors are, however, at the same time proved not to be so large that the methods employed, using only the fundamentals for the external circuit and the resultant effective values for the transductor, are not justified in view of their necessity in order to obtain a clear view of the physical processes and their approximate quantitive relations. As a matter of fact, the experimental verifications quoted in paragraph V show an agreement with the theoretical results obtained while neglecting the effect of harmonics, which may seem surprising in view of the high values of particularly the ratio k_p.

IV.4 Relation between transductor circuit and external circuit

The universal fundamental characteristics of the transductor, according to equations (32) and (33) as well as figures 30 and 31, yield a simple and practical means for expressing the properties of the transductor itself. When combining the fundamental characteristics with the load characteristics, as has been done in for instance in the figures 20 and 21, the load characteristics must, however, be

plotted from equations containing the proper coefficients to match the curves of the fundamental characteristics of the transductor, if these are presented in their universal form. As is easily derived from the equations (4) and (14) the appropriate equation of the load characteristics is:

$$I^* = \frac{N}{\alpha Z}\left[\frac{\omega NX}{\sqrt{2}\,\beta Z}\,U_L^* \pm \sqrt{U^2 - \frac{\omega^2 N^2 R^2}{2\,\beta^2 Z^2}\,U_L^{*2}}\right] = \tag{41}$$

$$= \frac{\omega N^2}{\sqrt{2}\,\alpha\beta Z}\left[\frac{X}{Z}\,U_L^* \pm \sqrt{U^{*2} - \frac{R^2}{Z^2}\,U_L^{*2}}\right]$$

the formula being given as an explicite solution for I^* in order to correspond directly to the shape of the equations (32) and (33).

V. Experimental verification

V.1 Basic data

In order to check the theoretical train of thoughts developed above a rather extensive series of experiments has been carried out in the laboratory of the Division of Electric Machinery at the Royal Institute of Technology, Stockholm. In the following selected examples of these series of measurements will be made subject to numerical examination and discussion.

The diagram of connections is shown in fig. 33.

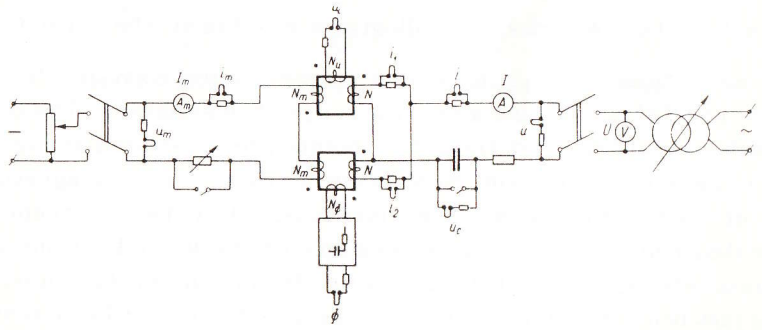

Fig. 33. Diagram of connections of test equipment for oscillographic measurements.

All the measurements and oscillographic records (except the oscillogram of fig. 48) were made with the same data of the equipment as were quoted earlier in connection with the examination of the agreement between theoretical and experimental curves. Below is given, for the sake of completeness, a table of numerical data:

Magnetization characteristic according to fig. 16.
Number of turns on a. c. side of transductor element $N = 860$.
D:o on d. c. side $N_m = 900$.
Resistance of the two a. c. windings in series $R_2 = 4{,}6\ \Omega$.
Series capacitance $C = 60\ \mu F$, which means $X = 53{,}1\ \Omega$.
Frequency $f = 50$ Hz.
Load resistance $R = 10{,}1\ \Omega$.
A. c. voltage (sinusoidal) $U = 15$, 20 and 25 V.

V.2 Experimental results

In fig. 34 are plotted the theoretical (lines and crosses), and experimental (circles) control characteristic corresponding to the supply voltage $U = 15$ V. They agree fairly well with respect to the range of modulation as well as to the ranges of stable equilibrium.

All the oscillograms presented in the following have the various quantities placed from top to bottom in the same order and were taken in the same scale. The succession of quantities and the results of calibration are seen from the oscillogram fig. 35, which also shows the general character of the time functions of the cited quantities. It was taken for the parameters $U = 20$ V, $I_m = 0{,}5$ A and for the working point lying on the upper branch of the control characteristic (see fig. 23 b).

For $U = 15$ V a series of oscillograms was taken, the current $\frac{U_m}{R_m}$ increasing from $0{,}065$ A to $0{,}37$ A, these values corresponding to points just below and just above the range of modulation. The states of stable equilibrium in these two points are illustrated in fig. 36. The remaining oscillograms were taken at values of the magnetizing current within the range of modulations. Only two of them are presented here, fig. 37 giving an example of stable modulations with the magnetizing current $0{,}18$ A, and fig. 38 showing *unstable* modulations just below the upper limit of the range, the current being $0{,}36$ A. The reason for this instability will be discussed further below.

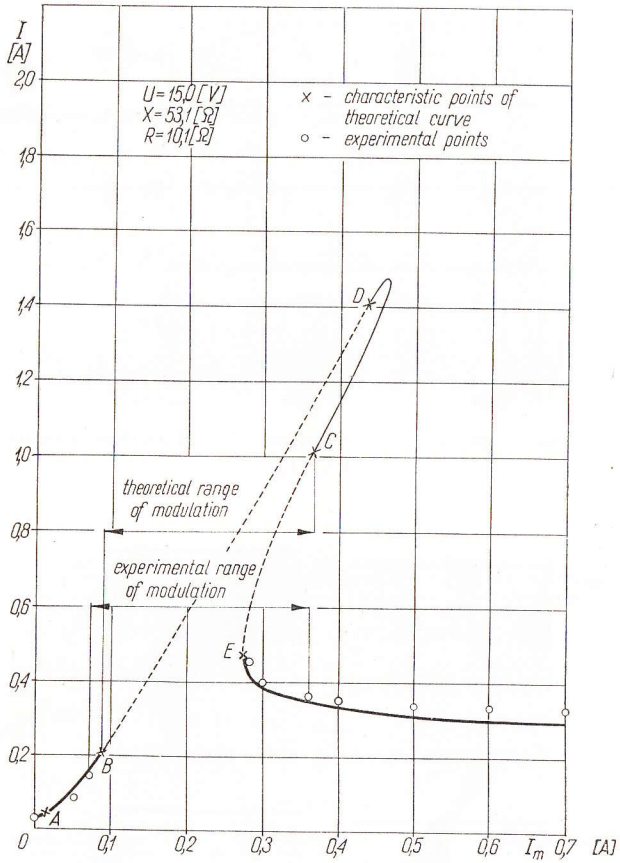

Fig. 34. Theoretical and experimental control characteristics.

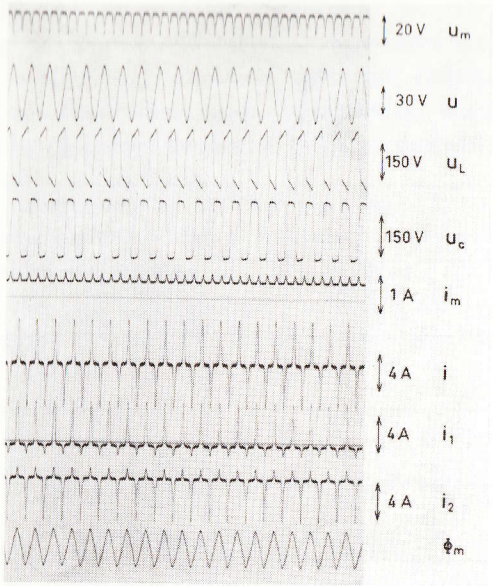

Fig. 35. Oscillogram showing voltages, currents, and flux during stable equilibrium. $U=20$ V; $I_m=0{,}5$ A.

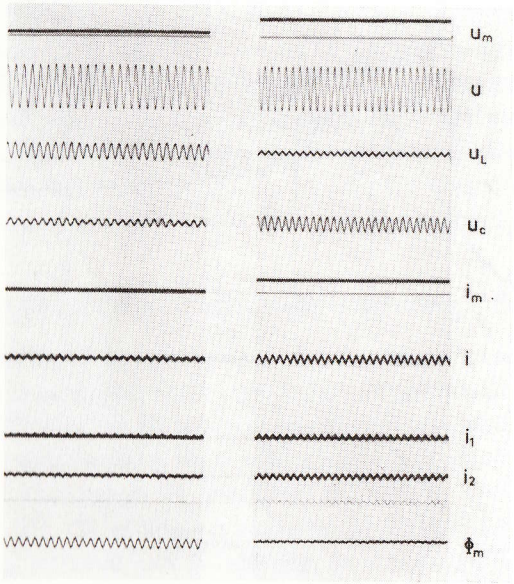

Fig. 36. Stable equilibrium just below and just above range of modulations. $U=15$ V; $I_m=0{,}065$ and $0{,}37$ A.

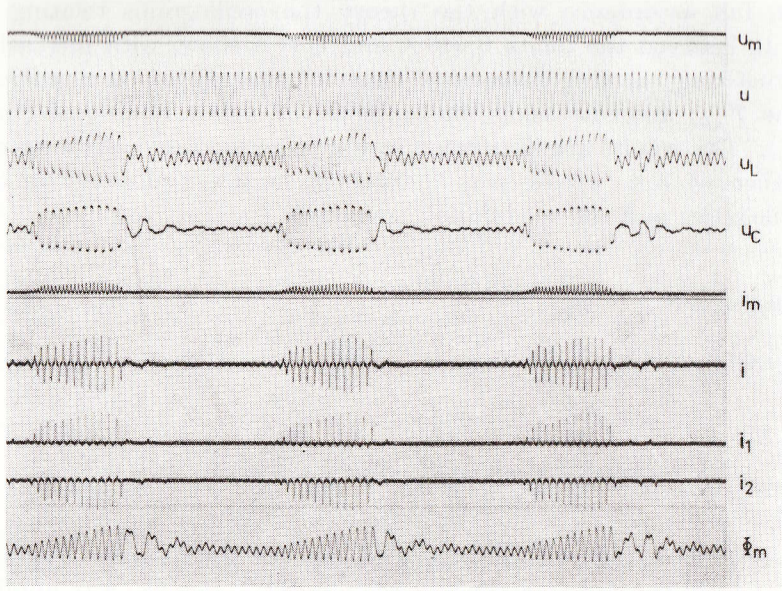

Fig. 37. Stable modulations. $U=15$ V; $I_m=0{,}18$ A.

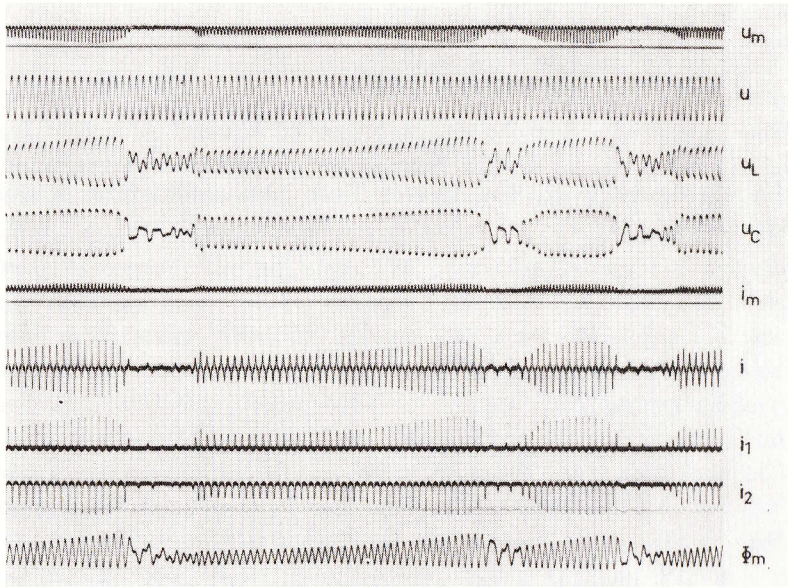

Fig. 38. Unstable modulations. $U=15$ V; $I_m=0{,}36$ A.

In full accordance with the theory the oscillograms relating to points between the limits 0,065 A and 0,37 A show, with increasing magnetizing current, decreasing time interval of low a. c. current (time T_{AB}) and increasing time interval of high a. c. current (time T_{CD}). The results are illustrated in the following table, showing the number of a. c. cycles per interval, as counted directly on the oscillogram, and the modulation frequency f_m.

Oscillogram	$\frac{U_m}{R_m}$	$50\ T_{AB}$	$50\ T_{CD}$	$f_m = \frac{1}{T_{AB} + T_{CD}}$
	A	cycles		Hz
Fig. 37	0,07	57	10	0,75
	0,18	23	12	1,43
	0,29	13	17	1,67
Fig. 38	0,36	6—10	14—44	2,50—0,93

As a check the method of computing the time values T_{AB} and T_{CD} which has been exposed in section III.7, fig. 28, was applied on the case illustrated in fig. 37. The actual numerical conditions are shown in fig. 39. The surface above the abscissa axis gives $T_{AB} = 0,42$ and the surface below that axis $T_{CD} = 0,26$. This means:

$$\begin{cases} 50\ T_{AB} = 21 \\ 50\ T_{CD} = 13 \\ f_m = \dfrac{1}{T_{AB} + T_{CD}} = 1,47 \end{cases}$$

The agreement with the figures from the oscillogram is quite satisfactory.

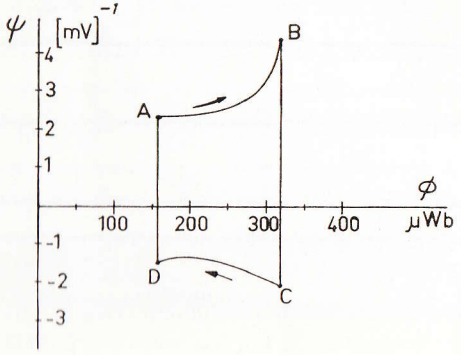

Fig. 39. Graph for calculation of time intervals from transformed stable limit cycle.

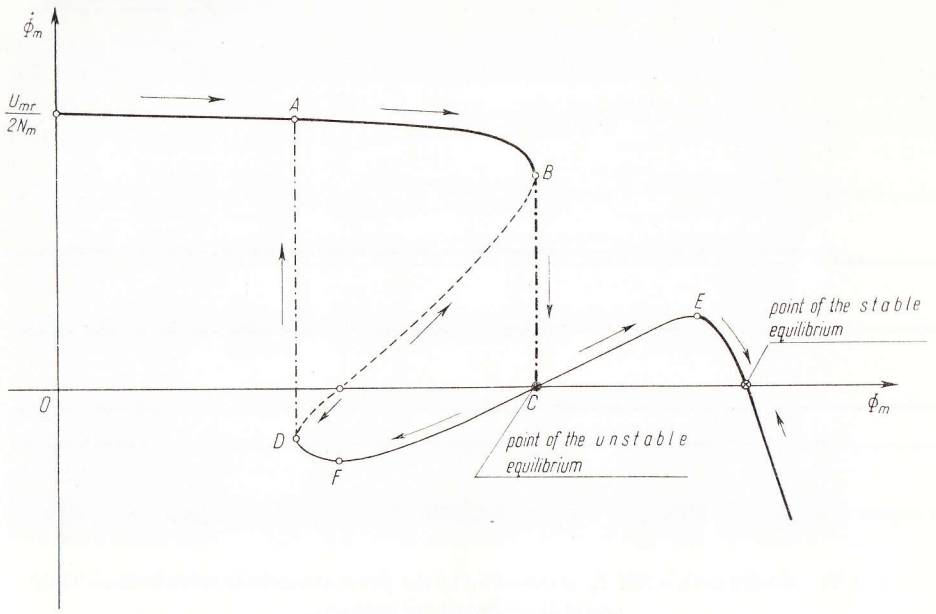

Fig. 40. Phase portrait explaining origin of unstable modulations.

To explain the instability of the modulation frequency for $\frac{U_m}{R_m} = 0,36$ A, i. e. for the current corresponding to the upper limit of the range of modulation, let us plot in qualitative form the phase portrait of the system, fig. 40. For these conditions, the system has two points of equilibrium: one stable, and one unstable (point C). From practical point of view, the operation in point C is possible only during a very short period of time, after which the working point must leave point C, passing either to the right, i. e. toward the point of stable equilibrium, or to the left, i. e. it will make one oscillation and then come back to point C. Of course, under such conditions, the frequency of modulations as well as the modulations themselves cannot be stable. This applies to any such case of limit magnetization current, where the right hand bottom, or the left hand top corner of the limit cycle corresponds to a point of unstable equilibrium, the time derivative $\dot{\Phi}_m$ being theoretically zero with positive derivative with respect to Φ_m.

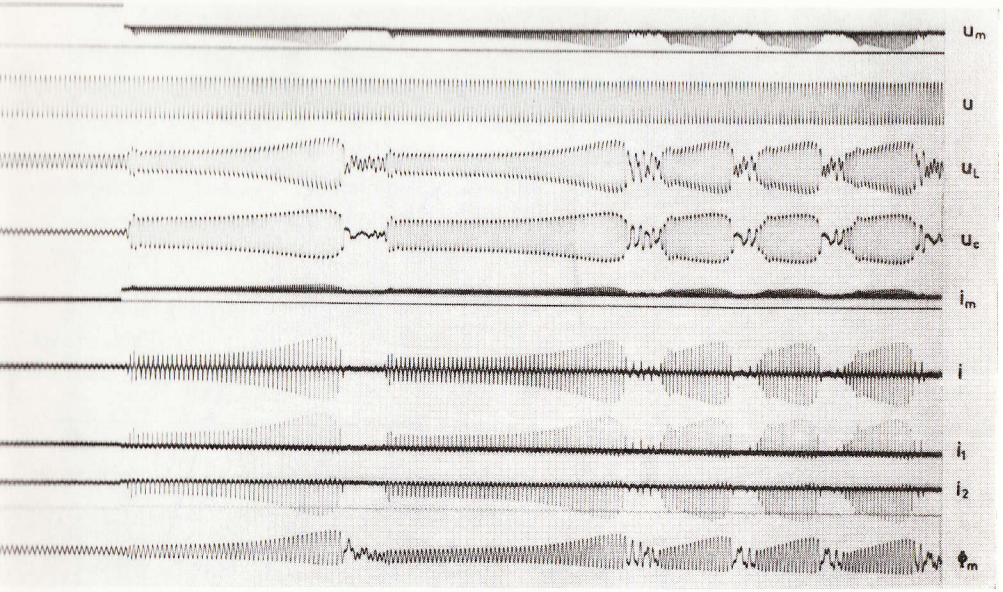

Fig. 41. Modulations when I_m is raised up to the point of unstable modulations. Only unstable modulations appearing.

The oscillogram fig. 38, referred to above, presents a case where the frequency of modulation varies, due to the explanation given, from 2,50 Hz to 0,93 Hz.

Very interesting are the oscillograms shown on fig. 41 and 42. They were taken under the same conditions, viz. for $U = 15$ V and for $\frac{U_m}{R_m}$ changed from 0,06 A to 0,36 A, i. e. to the value corresponding to the point of unstable equilibrium. In spite of the same conditions, in fig. 41 there is only a series of modulations of unstable frequency (like on fig. 38), while in fig. 42 we have got just after one period of modulation the spontaneous transition from the modulation range to the state of stable equilibrium. Physically, this transition was caused by some random fluctuations of the quantity $\frac{U_m}{R_m}$.

According to the theory presented above, the time intervals T_{BC} and T_{DA} of the modulation period are both equal to zero. The oscillograms of figs. 38 and 41 show, however, that this rule holds with some approximation only. Particularly during the transition from

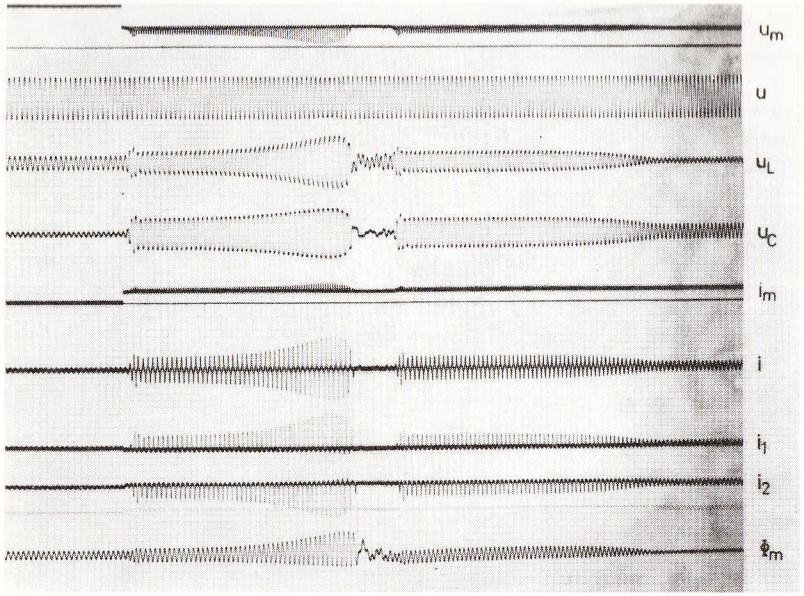

Fig. 42. Modulations when I_m is raised up to the point of unstable modulations. Stable equilibrium attained.

the interval of high currents to the interval of low currents, i. e. from point D to point A, there appear damped oscillations in voltages, currents and fluxes. The frequency of these oscillations is, of course, forced by the parameters of the a. c. circuit of fig. 33. Generally, the character of transitions from point B to C, and from D to A, or shortly the character of jumps during modulations, is of exactly the same character as the jumps observed in the usual ($I_m = 0$) ferro-resonance circuit. This property is confirmed by oscillograms presented on figs. 43 and 44, taken for $I_m = 0$, and for U changed from 0 to 75 V (fig. 43), and from 34 V to 0 (fig. 44), i. e. for the voltage U changed in such a way that it contains the values corresponding to the points of jumps, viz. $U = 74$ V and $U = 20$ V respectively.

The transition from the modulation range to the state of stable equilibrium is shown by the oscillogram of fig. 45. It was taken for the constant value of the current $\frac{U_m}{R_m} = 0,25$ A, and for the voltage U raised from 15 V to 20 V. The phenomenon is in full agreement with what could be expected from fig. 24 b.

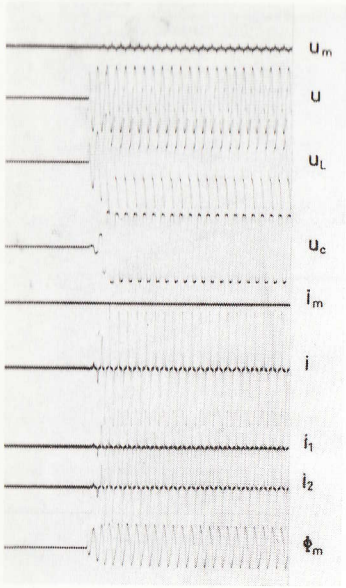

Fig. 43. Jump when regulating voltage U to cause transition from low to high current. $I_m = 0$.

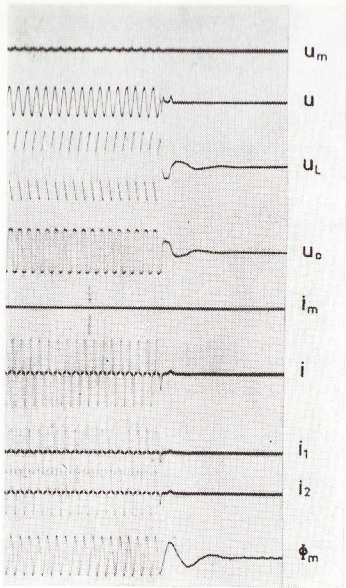

Fig. 44. Jump when regulating voltage U to cause transition from high to low current. $I_m = 0$.

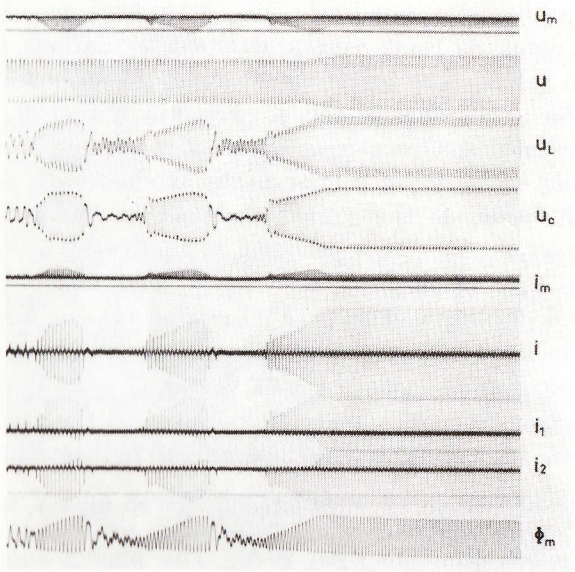

Fig. 45. Transition from modulation to stable equilibrium.

The oscillograms of figs. 46 and 47 were taken for the constant value of the voltage $U = 20\,\mathrm{V}$ and for the current $\frac{U_m}{R_m}$ changed in the first case from $0{,}50\,\mathrm{A}$ to $0{,}70\,\mathrm{A}$ and in the second case from $0{,}35\,\mathrm{A}$ to $0{,}25\,\mathrm{A}$. In both cases the initial conditions were chosen in such a way that during the transients the working point should pass through the region of negative inductance of control windings (see fig. 24). Fig. 22 gives a clear explanation of the lowering of the current I in the first case, and its rising in the second case. Generally, the character of transients agrees very well with the theoretical time characteristics which may be predicted from figs. 22 and 24.

Particularly interesting is the oscillogram presented in fig. 48. It refers to the load resistance $R = 17{,}4\,\Omega$. The value of capacitance was kept on the unchanged level ($X = 53{,}1\,\Omega$). The oscillogram was taken for the constant value of $U = 33{,}5\,\mathrm{V}$ and with $\frac{U_m}{R_m}$ raised slowly, at approximately constant rate, from 0 up to $0{,}7\,\mathrm{A}$. It gives a clear illustration of the case where the magnetization characteristic of control windings is of the type presented in fig. 27 a. Indeed, contrary to the oscillograms presented on figs. 36 and 42 the range of modulation is in this case succeeded by a range of stable work with the load current being of the order of magnitude of the resonance current $\left(I \approx I_{\max} = \frac{U}{R}\right)$.

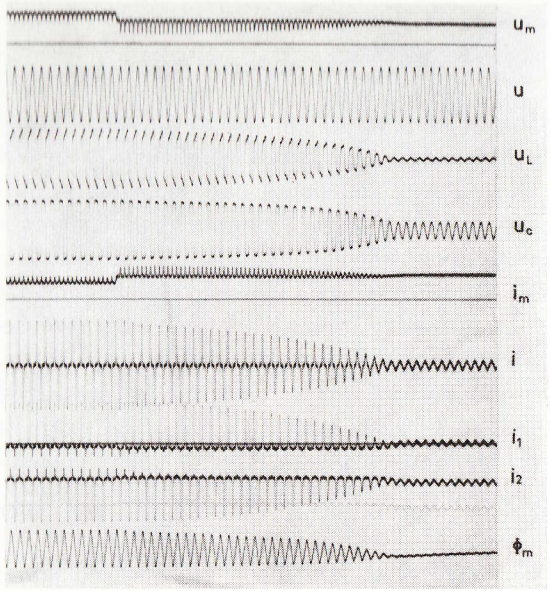

Fig. 46. Transition between points of stable equilibrium where the transient has to pass region of negative inductance of control windings. $\frac{U_m}{R_m}$ raised.

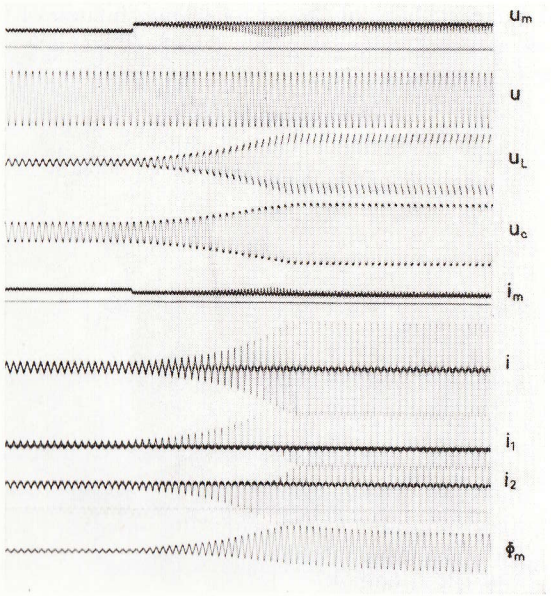

Fig. 47. Transition between points of stable equilibrium where the transient has to pass region of negative inductance of control windings. $\frac{U_m}{R_m}$ lowered.

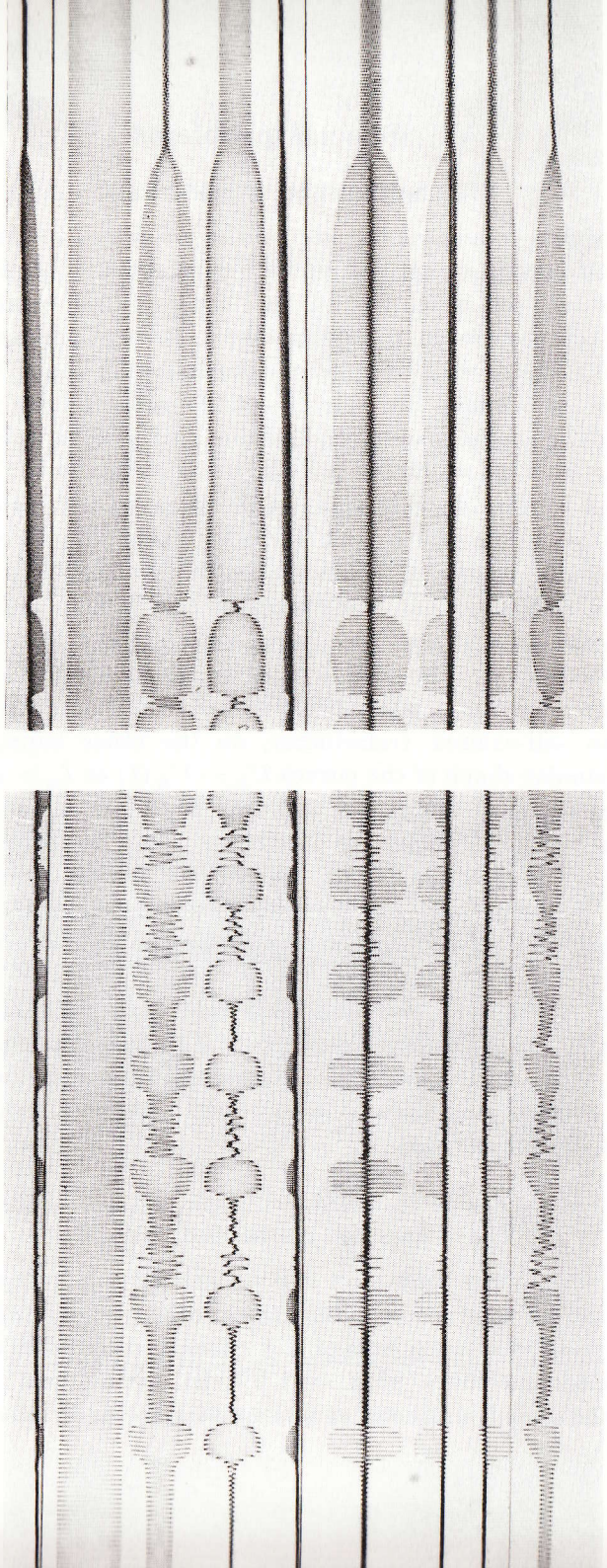

Fig. 48. Series of stable modulations succeeded by stable equilibrium in the neighbourhood of resonance.

VI. Special problems

VI.1 Self-excited transductors

The preceding treatment has been entirely confined to transductors without self-excitation. If self-excitation exists, and particularly in the case of auto self-excitation, i. e. at 100 per cent self-excitation, the condition for occurrence of self-sustained modulations are far less favourable. This is understood from the following reasoning:

Consider for example the case $U = 15$ V in the figures 22 b, 23 b and 24 b. The stable limit cycle, creating modulations, is due to the sign of the slope of the curve section $B—D$ in fig. 24 b. This slope is governed by the opposite signs of the slope of the corresponding curve sections in the figures 22 b and 23 b. This difference is on the other hand due to the different shapes of the fulldrawn curves in the figures 20 b and 21 b, the curves in the former case having a point of inflexion and a steeply rising section, which is not the case for the latter curves. The steeply rising section is due to the "current transformer effect" of a transductor without self-excitation.

An auto self-excited transductor, on the other hand, shows a mutually similar shape of the curves $U_L = U_L(I)$ at $I_m = \text{const.}$ and the curves $U_L = U_L(I)$ at $\Phi_m = \text{const.}$ Both are of the type corresponding to fig. 21 b. In this case there would not have been any section $B—D$ of the curves in the figures 22 b and 23 b having opposite signs of their slope, and consequently no section $B—D$ in fig. 24 b with a slope of the type necessary for the creation of a stable limit cycle.

Practical tests have also confirmed that auto self-excited transductors only in very special cases give rise to self-sustained modulations. They are consequently to be preferred when such modulations are to be avoided, and have to be left out of consideration when the modulation effect is desired.

VI.2 Capacitor in the d. c. circuit

Fig. 49 shows the diagram of connections of an arrangement frequently used for intermittent illumination of show-windows etc. The general type of the time curves of a. c. current, rectified d. c. voltage, and capacitor current is illustrated by the oscillograms in fig. 50, taken on the same transductor as was used for the experiments quoted

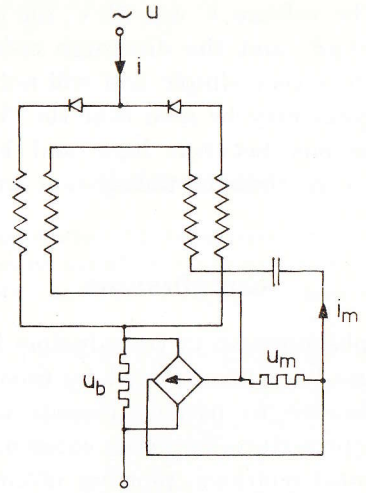

Fig. 49. Diagram of connections of modulating device using capacitor in d. c. circuit.

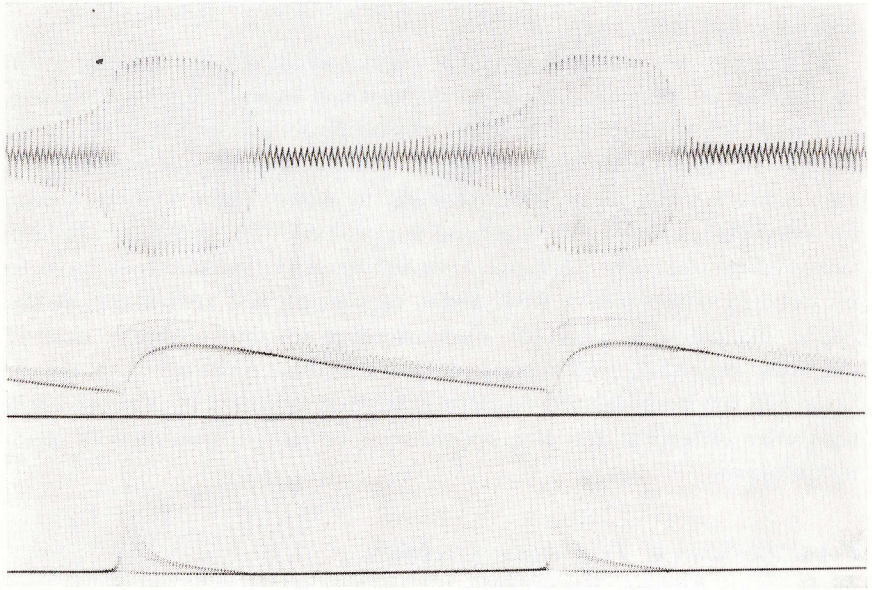

Fig. 50. Modulations created by capacitor in d. c. circuit.

in the preceding. The voltage U was 55 V, the load resistance 60 Ω, the capacitance 450 μF, and the discharge resistance 4 000 Ω. The theory of the system is very simple and will not be dealt with here.

From the oscillogram may be seen that the "impulse effect", that is the sharp transitions between high and low current, is less pronounced in this case than in the system with capacitor in the a. c. circuit.

Conclusions

The modulation phenomenon in transductors having capacitors in their a. c. circuits has been investigated by theory and experiments, with particular reference to parallel transductors of the non self-excited type. By a procedure involving experimental measurements of certain fundamental relations, plotting of combined curves, and physical considerations, a clear explanation of the phenomena has been attained. This procedure is based on certain approximations with respect to the influence of harmonics. Experimental verifications, mainly by means of oscillograms, have, however, proved good agreement between actual results and conclusions from the theoretical reasoning.

A purely mathematical method, employing Bessel functions, has been briefly indicated.

It has also been shown that the results obtained are equally valid in the case of series transductors without self-excitation. Self-excited, and particularly auto self-excited, transductors are on the other hand far less favourable for use in circuits where modulations are desired, and consequently more advantageous in cases where any tendency for creating modulations must be suppressed. In practical applications where for other reasons non self-excited transductors have to be used in combination with series capacitors the treatment in the paper furnishes a basis for dimensioning so as to obtain desired qualities regarding self-sustained modulations, although the conditions are too complicated to permit the formulation of a simple and universal criterium for the appearance or non-appearence of such modulations.

Royal Institute of Technology, Stockholm,
Division of Electric Machinery,
June 1959.

References

Bessonov, L. A. The computation of ferroresonance circuits with d. c. pre-saturated reactors and magnetic amplifiers. Sbornik statey po avtomatike i elektrotekhnike, Isdatelstvo Akademii Nauk SSSR, Moscow, 1956, p. 221—230 (in Russian).

Bogolyubov, V. E. The quasi-relaxation oscillations in ferroresonance circuits with d. c. pre-saturation, Elektrichestvo, Nr 6, 1949, p. 42—46 (in Russian).

Bogolyubov, V. E. The computation of the quasi-relaxation oscillations in ferroresonance circuits with d. c. pre-saturated reactors, Elektrichestvo, Nr 8, 1951, p. 64—68 (in Russian).

Johnson, W. C. and Latson, F. W. An analysis of transients and feedback in magnetic amplifiers, AIEE Transactions, Vol. 69, 1950, p. 604—612.

Ładziński, R. J. An outline of the theory of transductor, Zeszyty Naukowe, Politechniki Warszawskiej — Elektryka, Nr 1, 1953, p. 21—57 (in Polish).

Truxal, J. G. Automatic feedback control system synthesis, Mc Graw-Hill, New York, 1955, p. 615—631.

Kümmel, F. Verstärkung kleiner Wechselspannungen mit dem magnetischen Verstärker, ETZ-A. H. 11, Juni 1954, p. 367—372.

Table of contents

KUNGL. TEKNISKA HÖGSKOLANS HANDLINGAR

TRANSACTIONS OF THE ROYAL INSTITUTE OF TECHNOLOGY
STOCKHOLM, SWEDEN

Nr 148 1959

Electrical Engineering 3

UDC 621.318.435.3

SELF-SUSTAINED MODULATIONS IN TRANSDUCTOR CIRCUITS WITH SERIES CAPACITORS

BY

F. DAHLGREN and R. ŁADZIŃSKI

GÖTEBORG 1959
ELANDERS BOKTRYCKERI AKTIEBOLAG

Förteckning över

KUNGL. TEKNISKA HÖGSKOLANS HANDLINGAR

Fullständig förteckning finnes i samtliga häften upp till nr 145.

Complete list to be found in all issues up to nr 145.

51. DAHLGREN, F., *Theory and Applications of Wave Vectors.* 68 s. 1951. Kr. 7: 50.
52. LARSSON, GERHARD, *Income Value of Marginal Areas on Farms.* 61 s. 1951. Kr. 7: —.
53. DAHLGREN, F., and BIRINGER, P., *Speed Regulation of Slip-Ring Induction Motors for Special Purposes.* 39 s. 1951. Kr. 4: 50.
54. WIDELL, T. A., and JUHÁSZ, S. I., *Metal Temperature in Regenerative and Recuperative Air Preheaters.* 50 s. 1952. Kr. 6: 50.
55. FANT, GUNNAR, *The Heterodyne Filter.* 78 s. 1952. Kr. 10: —.
56. VOIPIO, ERKKI, *Voltage Stability of Synchronous Alternators with Capacitive Loads.* 64 s. 1952. Kr. 8: —.
57. NIORDSON, FRITHIOF I. N., *Transmission of Shock Waves in Thinwalled Cylindrical Tubes.* 24 s. 1952. Kr. 3: 50.
58. MEYERSBERG, G., *Grösseneinfluss und Randeinfluss auf die Festigkeit der Werkstoffe.* 123 s. 1952. Kr. 12: —
59. BJÖRLING, G., *The Conductivity of some Molten Silicates on Fayalite Basis.* 32 s. 1952. Kr. 4: —.
60. BRUNDELL, P.-O. and ENANDER, B., *The Neutron-Proton System with a Central Exponential Potential,* I. 14 s. 1952. Kr. 3: —.
61. WINQVIST, GUSTAF, *Ground Water in Swedish Eskers.* 91 s. 1953. Kr. 10: —.
62. PETERSSON, S., *Investigation of Stress Waves in Cylindrical Steel Bars.* 22 s. 1953. Kr. 3: 50.
63. TISCHER, F., *The Effective Bandwidth of Video Amplifiers.* 32 s. 1953. Kr. 4: —.
64. FALKEMO, CURT, *On the Possibilities of Estimating the Towing Resistance of Ships by Tests with Small Models.* I. (Publication No 2 of the Ship Testing Laboratory.)
65. PRAGER, WILLIAM, *A Geometrical Discussion of the Slip Line Field in Plane Plastic Flow.* 27 s. 1953. Kr. 4: —.
66. ODQVIST, FOLKE K. G., *Influence of Primary Creep on Stresses in Structural Parts.* 18 s. 1953. Kr. 2: 50.
67. ALM, EMIL, *Small Self-excited and Selfcompounded Three-phase Generators.* 42 s. 1953. Kr. 6: —.
68. HÁMOS, L. v., *An X-ray Microanalyzer Camera* 68 s. 1953. Kr. 9: —.
69. KNUDSEN, NIELS H., *Abnormal Oscillations in Electric Circuits Containing Capacitance.* 134 s. 1953. Kr. 12: —.
70. ALLANDER, CLAES GUSTAF, *Untersuchung des Adsorptionsvorganges in Adsorbentenschichten mit linearer Adsorptionsisotherme.* 160 s. 1953. Kr. 10: —.
71. RAHM, LENNART, *Flow Problems with Respect to Intakes and Tunnels of Swedish Hydro-Electric Power Plants.* 219 s. 1953. Kr. 18: —.
72. NILSSON, SVEN GÖSTA, *The Motion of Electrons in Two Combined Magnetic Fields.* 23 s. 1953. Kr. 4: —.
73. NIORDSON, FRITHIOF I. N., *Vibrations of a Cylindrical Tube Containing Flowing Fluid.* 28 s. 1953. Kr. 4: —.
74. SCHNITTGER, JAN R., *Vortex Flow in Axial Turbo Machines.* 62 s. 1954. Kr. 8: —.
75. VON DARDEL, G. F., *The Interaction of Neutrons with Matter Studied with a Pulsed Neutron Source.* 104 s. 1954. Kr. 10: —.
76. HELLSTRÖM, B., and RUNDGREN, L., *Model Tests on Ölands Södra Grund Lighthouse.* 66 s. 1954. Kr. 8: —.
77. BROWN, GÖSTA, *Theory of Moist Air Heat Exchangers.* 33 s. 1954. Kr. 5: —.
78. FORSSELL, CARL, *Schubfestigkeit und Schubbewehrung der Betonbalken.* 65 s. 1954. Kr. 10: —.
79. *Basorganisation för forskning vid de tekniska högskolorna.* 154 s.+6 tabellbilagor. 1954. Kr. 12: —. (Not for exchange.)
80. BJÖRKMAN, J., and LINDBERG, L., *Development of trochotrons.* 131 s. 1954. Kr. 12: —.
81. WOXÉN, R., *Högre teknisk utbildning och teknisk-vetenskaplig forskning i Storbritannien och Nederländerna.* 69 s. 1954. Kr. 7: —.
82. ENHAMRE, ERIK, *Effects of Underwater Explosions on Elastic Structures in Water.* 79 s. 1954. Kr. 9: —.
83. KIVISILD, HANS R., *Wind Effect on Shallow Bodies of Water with Special Reference to Lake Okeechobee.* 146 s. 1954. Kr. 15: —.
84. ÖSTLUND, LARS, *Lateral Stability of Bridge Arches Braced with Transverse Bars.* 124 s. 1954. Kr. 12: —.
85. ÅSLANDER, ALFRED, *An Attempt to Solve the Phosphate Problem in Crop Production so as to Economize with the World Supply of Phosphates.* 64 s. 1954. Kr. 8: —.
86. KARLQVIST, OLLE, *Calculation of the Magnetic Field in the Ferromagnetic Layer of a Magnetic Drum.* 28 s. 1954. Kr. 3: 50.
87. THORÉN, H. BERTIL, *Synthetic Methods for Interruption Tests on Circuit-Breakers.* 61 s. 1955. Kr. 7: —.
88. SVENSSON, JONAS, *A New Formula for Particle Size Distribution of Products Produced by Comminution.* 53 s. 1955. Kr. 6: —.
89. HALLÉN, ERIK, *Further Investigations into Iterated Sine- and Cosine-Integrals and their Amplitude Functions with Reference to Antenna Theory.* 44 s. 1955. Kr. 6: —.

Forts. å omsl. 3:dje sida.